Structural Engineering and Mechanics, *Vol. 73, No. 5 (2020) 565-584*
DOI: https://doi.org/10.12989/sem.2020.73.5.565

Thermo-electro-elastic nonlinear stability analysis of viscoelastic double-piezo nanoplates under magnetic field

Farzad Ebrahimi*[1], S. Hamed S. Hosseini[1] and Rajendran Selvamani[2]

[1]*Department of Mechanical Engineering, Faculty of Engineering, Imam Khomeini International University, Qazvin, Iran*
[2]*Department of mathematics, Karunya Institute of Technology and Sciences, Coimbatore, India*

(Received June 12, 2018, Revised July 18, 2019, Accepted August 27, 2019)

Abstract. The nonlinear thermo-electro-elastic buckling behavior of viscoelastic nanoplates under magnetic field is investigated based on nonlocal elasticity theory. Employing nonlinear strain-displacement relations, the geometrical nonlinearity is modeled while governing equations are derived through Hamilton's principle and they are solved applying semi-analytical generalized differential quadrature (GDQ) method. Eringen's nonlocal elasticity theory considers the effect of small size, which enables the present model to become effective in the analysis and design of nano-sensors and nano actuators. Based on Kelvin-Voigt model, the influence of the viscoelastic coefficient is also discussed. It is demonstrated that the GDQ method has high precision and computational efficiency in the buckling analysis of viscoelastic nanoplates. The good agreement between the results of this article and those available in literature validated the presented approach. The detailed mathematical derivations are presented and numerical investigations are performed while the emphasis is placed on investigating the effect of the several parameters such as electric voltage, small scale effects, elastomeric medium, magnetic field, temperature effects, the viscidity and aspect ratio of the nanoplate on its nonlinear buckling characteristics. It is explicitly shown that the thermo-electro-elastic nonlinear buckling behavior of viscoelastic nanoplates is significantly influenced by these effects. Numerical results are presented to serve as benchmarks for future analyses of viscoelastic nanoplates as fundamental elements in nanoelectromechanical systems.

Keywords: small scale effect; nonlinear buckling; double nanoplate; viscoelastic; GDQ

1. Introduction

In recent years, due to the instinct electro-mechanical coupling effects, piezo- electric materials have various practical applications in smart structures and systems (Kane and Mele (1997), Maiti *et al*. (2002)). Development of these nanostructures requires a good understanding of their properties such as vibration behavior. Nanoplates are two-dimensional structure of nano-scale size. Researches in these structures are increasing every day. The problem of buckling of thick plates has attracted considerable attention in recent years. Up to now, several researches have been conducted on the buckling characteristics of nanoplates. Most of the previous studies in the analysis of buckling indicated these studies are only limited in the linear buckling analysis of structures. In several investigations (Dickinson (1978), Sciuva (1986), Chattopkdhyay and Hadzhong (1994), Shahwan and Waas (1998), Ziliukas (2008), Moon and Yih (1968)), computed the buckling of plates by classical and higher order plate theory without considering the nonlinear terms in the governing equations.

In general, there are different kinds of methods including analytical and numerical ones for considering buckling of structures nanostructures. Finite element (FE) and differential quadrature method (DQM) in numerical methods have a good agreement with analytical methods. Javaheri and Eslami (2002) investigated thermal effect in buckling of functionally graded (FG) plates based on the classical plate theory. To study the elastic buckling behavior of orthotropic small-scale plates under biaxial compression, Murmu and Pradhan (2009) employed semi-analytical. To obtain the buckling response of single-layered graphene sheets (SLGS), Pradhan and Murmu (2010) employed DQM. In this work, both Winkler-type and Pasternak-type foundation models are employed to simulate the interaction between the graphene sheet and the surrounding elastic medium. Murmu *et al*. (2013) also investigated the buckling behavior of double nanoplates using an analytical method. In this work, they are reported the linear buckling characteristics of double layered nanoplates without considering the thermo-electro-elastic response. Ansari *et al*. (2011) developed a nonlocal elastic shell model to investigate the axially compressed buckling response of multi-walled carbon nanotubes (MWCNTs) considering thermal environment effect. Surface and piezoelectric effects on the buckling of piezoelectric nanofilms due to mechanical loads are studied by Zhang *et al*. (2014). The buckling analysis of functionally graded carbon nanotube-reinforced composite (FG-CNTRC) plates under various in-plane mechanical loads presented Lei *et al*. (2013). Recently, Young *et al*. (2014) used a modified couple stress theory for buckling analysis of sigmoid functionally graded material (S-FGM) nanoplates on elastic medium. Analysis of biaxial buckling behavior of double-orthotropic

*Corresponding author, Ph.D.
E-mail: febrahimy@eng.ikiu.ac.ir

ISSN: 1225-4568 (Print), 1598-6217 (Online)

microplate system including in-plane magnetic field, using strain gradient theory are presented by Jamalpoor and Hosseini (2015).

Recently, buckling of magneto-electro-elastic nanoplate is investigated based on nonlocal Mindlin theory by Li *et al*. (2014). However, the studies of mentioned above are only limited in the linear buckling analysis of structures and nanostructures. In 1973, based on nonlinear von Karman equations, Knightly and Sather (1974) developed nonlinear buckling of rectangular plate with using analytical method. Nonlinear bending analysis for a simply supported, shear deformable composite laminated plate subjected to combined uniform lateral pressure and compressive edge loads and resting on a two-parameter (Pasternak-type) elastic foundation is presented by Shen (2000). Kapania and Yang (1987) investigated nonlinear buckling, Postbuckling isotropic and laminated thin plates. They used the finite-element method. Based on von Karman's plate theory and Hamilton's principles, analysis of the nonlinear thermal post-buckling of a heated orthotropic annular plate is presented by Li *et al*. (2002). Based on the classical nonlinear von Karman plate theory, Ma and Wang (2003) also studied axisymmetric large deflection bending of a FG circular plate under mechanical, thermal and combined thermal–mechanical loadings. Recently, Kolahchi *et al*. (2015) investigated nonlocal nonlinear buckling analysis of embedded polymeric temperature-dependent microplates resting on an elastic matrix as orthotropic temperature-dependent elastomeric medium. In this work, they are reported the nonlinear buckling behaviors of single viscoelastic microplates without considering the electro-elastic response.

Therefore, the thermo-electro-elastic nonlinear buckling analysis of the double layered viscoelastic nanoplate has not been accomplished so far. In the present study, the mentioned task is accomplished, including the following novelties:

- Assessment of effects of using the electric field on the behavior of the double viscoelastic nanoplate, for the first time.
- The effects of electric voltage and magnetic field on the nonlinear buckling analysis of the double nanoplate with viscoelastic effect based on Kelvin-Voigt model, for the first time.
- A comprehensive parametric study including evaluation of effects of the small scale, elastomeric foundation, the viscidity and aspect ratio of the nanoplate.
- The presented conclusions extend the available published information regarding the double layered viscoelastic nanoplates and provide more accurate results for the more complicated viscoelastic nanoplate with elastomeric foundation.

Moreover, the tricky empirical experiments have always been a barrier in front of the new explorations; however employing intelligence solutions are one of the practical ways to address these issues. Whereas, artificial intelligence techniques have perfomed on a variety of experimental studies and proved to be reliable not only in case of parameters estimation but also the prediction of crucial design characteristics (Chuanhua Xu 2019, Shariati *et al.* 2019b, Shariati *et al.* 2019c, Trung *et al.* 2019, Armaghani *et al.* 2020, Shariati *et al.* 2020c, Shariati *et al.* 2020e, Shariati *et al.* 2020f). Different kind of algorithms has introduced which have their traits and advantages (Mohammadhassani *et al.* 2013, Mohammadhassani *et al.* 2015, Shao *et al.* 2019a, Shao *et al.* 2019b, Shi *et al.* 2019a, Suhatril *et al.* 2019, Shariati *et al.* 2020a, Shariati *et al.* 2020b, Shariati *et al.* 2020d). Using the relevant algorithms in order to analytical assessment has been carried out on different types of studies (Shao *et al.* 2015, Shahabi *et al.* 2016, Chahnasir *et al.* 2018, Sedghi *et al.* 2018, Shao *et al.* 2018, Katebi *et al.* 2019, Luo *et al.* 2019, Mansouri *et al.* 2019, Milovancevic *et al.* 2019, Shariati *et al.* 2019a, Shi *et al.* 2019b). That being the case, performing the artificial intelligence algorithms is a potential method to avoid non-linearity and sophisticated analysis of the nanoscale problems.

2. Formulation

Fig. 1 illustrates the double layered piezo nanoplate with the length a, width b and thickness h. in this work, the nanoplates are assumed to be homogeneous and isotropic. Unlike the conventional local elasticity, in the nonlocal elasticity theory it is assumed that the stress at a point is a function of strains at all points in the continuum (Eringen (1972), Eringen (1983)). According to the nonlocal elasticity theory, the basic equations for Hookean piezoelectric solids neglecting the body force are expressed by the following relationships

$$\sigma_{ij} = \int_V K(|X' - X|, \tau) \left[c_{ijkl}\varepsilon_{kl}(X') - e_{kij}E_k(X') - \lambda_{ij}\Delta T\right] dX' \quad (1)$$

$$D_i = \int_V K(|X' - X|, \tau) \left[e_{ikl}\,\varepsilon_{kl}(X') + \kappa_{kij}E_k(X') + p_i\Delta T\right] dX' \quad (2)$$

$$\sigma_{ij} = \rho\ddot{u}_i, \qquad D_{i,j} = 0. \quad (3a, 3b)$$

$$\varepsilon_{ij} = \tfrac{1}{2}\left(U_{i,j} + U_{j,i}\right), \quad E_i = -\Phi_{,i}. \quad (4a, 4b)$$

where $\sigma_{ij}, \varepsilon_{ij}, D_i, E_i, U_i$ and Φ are the components of the non-local stress tensor, strain tensor, electric displacement vector, electric field vector, displacement vector and electric potential, respectively. And $K(|X' - X|)$ is the Kernel function represents the nonlocal modulus. Also terms $c_{ijkl}, e_{kij}, \kappa_{kij}, \lambda_{ij}, p_i$ and ρ are the components of a fourth order elasticity tensor, piezoelectric constants, dielectric constants, thermal moduli, pyroelectric constants and mass density, respectively. ΔT denote the temperature difference between the top and bottom layers of the nanoplate. Eringen (1972) demonstrated that it is possible to represent the integral constitutive relation in an equivalent differential form as

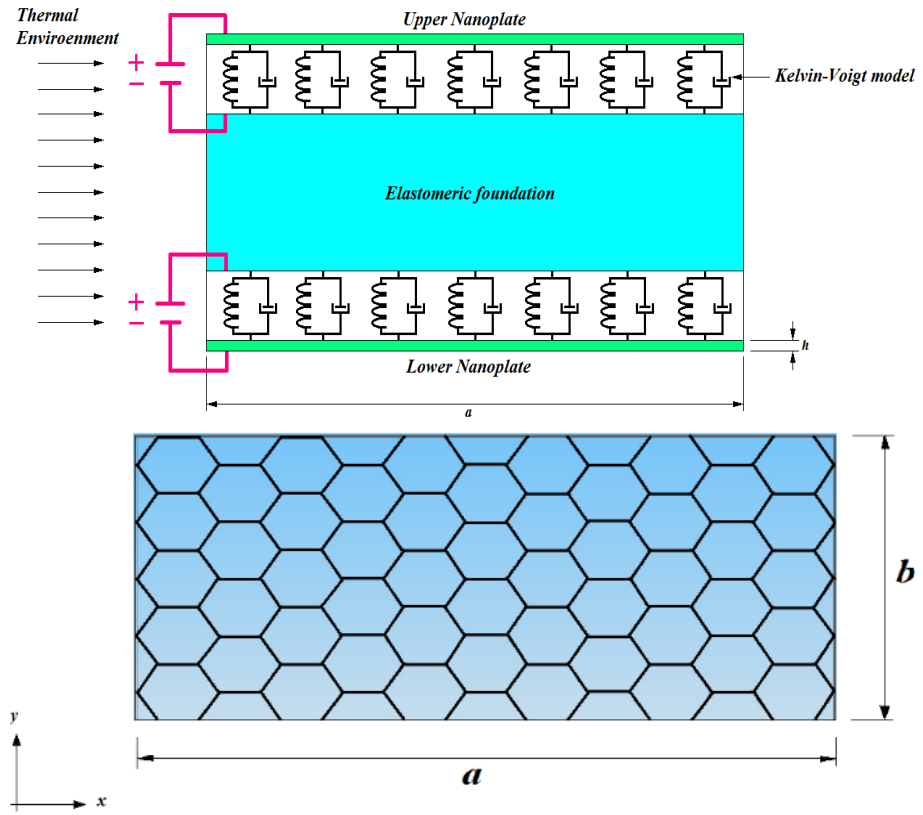

Fig. 1 double layered viscoelastic piezo-nanoplate embedded on an elastomeric medium

$$(1-\mu\nabla^2)\sigma_{ij} = c_{ijkl}\varepsilon_{kl} - e_{kij}E_k - \lambda_{ij}\Delta T$$
$$(1-\mu\nabla^2)D_i = e_{ikl}\,\varepsilon_{kl} + \kappa_{kij}E_k + p_i\Delta T \qquad (5a, b)$$

where , $\nabla^2 = \frac{\partial^2}{\partial x^2} + \frac{\partial^2}{\partial y^2}$ the Laplacian operator and $\mu = (e_0 a)$ is the nonlocal parameter, in which, a and e_0 are an internal characteristic length and a constant that appropriates to each material, respectively. The value of e_0 needs to be determined from experiments or by matching the dispersion relation of plane waves with those of atomic lattice dynamics.

Based on classic elasticity theory, the displacement field of the CLPT is expressed as

$$U = u(x,y,t) - zw_{,x}$$
$$V = v(x,y,t) - zw_{,y} \qquad (6)$$
$$W = w(x,y,t)$$

In Eq. (6), U and V are the in-plane displacements of the plate along the x and y directions , W is the transverse displacement along the z direction, and u and v are the middle surface displacements along the x and y directions. Since the nonlinear vibration is assumed to have large amplitude motion, the von Karman type strain displacement relations are employed as

$$\varepsilon = \varepsilon_0 + z\kappa \qquad (7)$$

where ε is the strain vector, and ε_0 and κ can be expressed as

$$\varepsilon_0 = \begin{Bmatrix} u_{,x} + \frac{1}{2}w_{,x}^2 \\ v_{,y} + \frac{1}{2}w_{,y}^2 \\ u_{,y} + v_{,x} + w_{,x}w_{,y} \end{Bmatrix}, \qquad \kappa = \begin{Bmatrix} -w_{,xx} \\ -w_{,yy} \\ -2w_{,xy} \end{Bmatrix}. \qquad (8)$$

Now, we need to know the distribution of electric potent ial through the thickness of the PNP. In the investigation of piezoelectric nanobeams behavior, Ke and Wang (2012) ass umed that the electric potential distribution is a combination of a cosine and linear functions. Thus, following Ke and W ang (2012), the electric potential can be expressed as follow s

$$\Phi(x,y,z,t) = -\cos\left(\frac{\pi z}{h}\right)\phi(x,y,t) + \frac{2zV_0}{h}e^{i\omega t} \qquad (9)$$

where $\phi(x,y,t)$ is the electric potential of point $(x,y,0)$in the mid-plane at time t; V_0 is the external electric voltage; and ω denotes the complex eigenvalue. Using Eqs. (4b) and (9), the components of the electric field can be written as

$$E_x = \cos\left(\frac{\pi z}{h}\right)\frac{\partial\phi}{\partial x}, \qquad E_y = \cos\left(\frac{\pi z}{h}\right)\frac{\partial\phi}{\partial y},$$
$$E_z = -\frac{\pi}{h}\sin\left(\frac{\pi z}{h}\right)\phi - \frac{2V_0}{h}e^{i\omega t}. \qquad (10)$$

Using Eqs. (5), the non-local constitutive relations of thin PNP in the Cartesian coor dinates can be approximated as

$$\begin{Bmatrix}\sigma_{xx}\\ \sigma_{yy}\\ \sigma_{xy}\end{Bmatrix} - (\mu\,\nabla^2)\begin{Bmatrix}\sigma_{xx}\\ \sigma_{yy}\\ \sigma_{xy}\end{Bmatrix} = \begin{bmatrix}\tilde{c}_{11} & \tilde{c}_{12} & 0\\ \tilde{c}_{21} & \tilde{c}_{22} & 0\\ 0 & 0 & \tilde{c}_{66}\end{bmatrix}\begin{Bmatrix}\varepsilon_{xx}\\ \varepsilon_{yy}\\ 2\varepsilon_{xy}\end{Bmatrix} - \begin{bmatrix}0 & 0 & \tilde{e}_{31}\\ 0 & 0 & \tilde{e}_{31}\\ 0 & 0 & 0\end{bmatrix}\begin{Bmatrix}E_x\\ E_y\\ E_z\end{Bmatrix} - \begin{Bmatrix}\tilde{\lambda}_{11}\\ \tilde{\lambda}_{11}\\ 0\end{Bmatrix}\Delta T \tag{11}$$

$$\begin{Bmatrix}D_x\\ D_y\\ D_z\end{Bmatrix} - (\mu\,\nabla^2)\begin{Bmatrix}D_x\\ D_y\\ D_z\end{Bmatrix} = \begin{bmatrix}0 & 0 & 0\\ 0 & 0 & 0\\ \tilde{e}_{31} & \tilde{e}_{31} & 0\end{bmatrix}\begin{Bmatrix}\varepsilon_{xx}\\ \varepsilon_{yy}\\ 2\varepsilon_{xy}\end{Bmatrix} + \begin{bmatrix}\tilde{\kappa}_{11} & 0 & 0\\ 0 & \tilde{\kappa}_{11} & 0\\ 0 & 0 & \tilde{\kappa}_{33}\end{bmatrix}\begin{Bmatrix}E_x\\ E_y\\ E_z\end{Bmatrix} + \begin{Bmatrix}\tilde{p}_1\\ \tilde{p}_1\\ \tilde{p}_3\end{Bmatrix}\Delta T \tag{12}$$

All materials exhibit some viscoelastic response such as creep and relaxation (Lakes (2009)). Based on Kelvin-Voigt model (Lakes (2009), Findley (1976)), for a viscoelastic structure, elasticity tensor in Eq. (11), can be modified,

$$[c] = \begin{bmatrix}\tilde{c}_{11}\left(1+g\frac{\partial}{\partial t}\right) & \tilde{c}_{12}\left(1+g\frac{\partial}{\partial t}\right) & 0\\ \tilde{c}_{21}\left(1+g\frac{\partial}{\partial t}\right) & \tilde{c}_{22}\left(1+g\frac{\partial}{\partial t}\right) & 0\\ 0 & 0 & \tilde{c}_{66}\left(1+g\frac{\partial}{\partial t}\right)\end{bmatrix} \tag{13}$$

Where,

$$\tilde{c}_{11} = \tilde{c}_{22} = \frac{E}{1-\nu^2}\,, \qquad \tilde{c}_{12} = \tilde{c}_{21} = \frac{\nu E}{1-\nu^2}\,, \qquad \tilde{c}_{66} = \frac{E}{1+\nu}\,. \tag{14}$$

where E, υ, g and denote the Young's modulus, the Poisson's ratio, the viscoelastic structural damping coefficient, the coefficient of thermal expansion and the temperature difference between the top and bottom layers of the nanoplate, respectively. The following equilibrium equations can be expressed (Reddy (2010)). In Eqs. (11) and (12), $\tilde{c}_{ij}\,, \tilde{e}_{ij}\,, \tilde{k}_{ij}\,, \tilde{\lambda}_{ij}$ and $\tilde{p}_{ij}$ are respectively the reduced elastic constants, piezoelectric constants, dielectric constants, thermal moduli and pyroelectric constants for the piezoelectric nanoplate under the plane stress state (Zhao *et al*. (2006), Pietrzakowski (2008)). These constants are given as

$$\tilde{c}_{11} = c_{11} - \frac{c_{13}^2}{c_{33}}\,,\ \tilde{c}_{12} = c_{12} - \frac{c_{13}^2}{c_{33}}\,,\ \tilde{c}_{66} = c_{66}\,,\ \tilde{e}_{31} = e_{31} - \frac{c_{13}e_{33}}{c_{33}}, \tag{15}$$

$$\tilde{k}_{11} = k_{11}\,,\ \tilde{k}_{33} = k_{33} - \frac{c_{33}^2}{c_{33}}\,,\quad \tilde{\lambda}_{11} = \lambda_{11} - \frac{c_{13}\lambda_{33}}{c_{33}}\,,\ \tilde{p}_1 = p_1\,,\ \tilde{p}_3 = p_3 - \frac{e_{33}\lambda_{33}}{c_{33}}.$$

The total potential energy, V, of the double nanoplate is t he sum of strain energy, U and the work done by the elasto meric medium, W. The total strain energy of piezoelectric n anoplate (Π_s) can be expressed as,

$$\begin{aligned}\delta\Pi_s = \iiint_V \big(&\sigma_{xx}\,\delta\varepsilon_{xx} + \sigma_{yy}\,\delta\varepsilon_{yy} + 2\sigma_{xy}\,\delta\varepsilon_{xy}\\ &- D_x\,\delta E_x - D_y\,\delta E_y - D_z\,\delta E_z\big)dV\\ &= \iint_A \Bigg[N_{xx}\frac{\partial\delta u}{\partial x} + N_{yy}\frac{\partial\delta v}{\partial y}\\ &+ N_{xy}\left(\frac{\partial\delta u}{\partial y} + \frac{\partial\delta v}{\partial x}\right)\\ &- \left(M_{xx}\frac{\partial^2\delta w}{\partial x^2} + M_{yy}\frac{\partial^2\delta w}{\partial y^2}\right.\\ &\left.+ 2M_{xy}\frac{\partial^2\delta w}{\partial x\partial y}\right)\Bigg]dA\\ &- \iint_A \int_{-\frac{h}{2}}^{\frac{h}{2}} \Big\{D_x\cos\left(\frac{\pi z}{h}\right)\frac{\partial\delta\emptyset}{\partial x}\\ &+ D_y\cos\left(\frac{\pi z}{h}\right)\frac{\partial\delta\emptyset}{\partial y}\\ &- D_z\frac{\pi}{h}\sin\left(\frac{\pi z}{h}\right)\delta\emptyset\Big\}dz\,dA\end{aligned} \tag{16}$$

Here, A is the area of the plate. The stress resultants N_{ij}, and the moment resultants, M_{ij}, for the nonlocal nanoplate can be defined as

$$\{N_{ij}, M_{ij}\} = \int_{-\frac{h}{2}}^{\frac{h}{2}} \sigma_{ij}(1,z)dz \qquad i = x,y \quad j = x,y \tag{17}$$

The external works are due to temperature-dependent, elastomeric medium and magnetic field. The wo rk done by elastic medium is calculated from

$$\delta W_f = \iint_A (P\ \delta w)\ dA \tag{18}$$

where P is related to orthotropic elastomeric medium. Orthotropic elastomeric foundation can be expressed as (Shen (2009), Kutlu and Omurtag (2012))

$$\begin{aligned}\mathrm{P} = \mathrm{k\,w} - \mathrm{G_\xi}\big(&\cos^2\theta\ \mathrm{w_{,xx}} + 2\cos\theta\sin\theta\ \mathrm{w_{,yx}}\\ &+ \sin^2\theta\ \mathrm{w_{,yy}}\big)\\ &- \mathrm{G_\eta}\big(\sin^2\theta\ \mathrm{w_{,xx}}\\ &+ 2\sin\theta\cos\theta\ \mathrm{w_{,yx}}\\ &+ \cos^2\theta\ \mathrm{w_{,yy}}\big)\end{aligned} \tag{19}$$

Where, angle θ describes the local ξ direction of

orthotropic foundation with respect to the global x-axis of the plate. Since the elastomeric medium is relatively soft, the foundation stiffness k may be expressed by

$$\begin{aligned} \mathrm{k} &= \frac{\mathrm{E}_0}{4\mathrm{L}(1-\mathrm{v}_0^2)(2-\mathrm{C})^2}[5 \\ &\quad -(2\gamma^2+6\gamma+5)\exp(-2\gamma)], \\ \mathrm{C} &= (\gamma+2)\exp(-\gamma)\ , \qquad \gamma = \frac{\mathrm{H_s}}{\mathrm{L}}, \\ \mathrm{E}_0 &= \frac{\mathrm{E_s}}{(1-\mathrm{v_s^2})}\ , \quad \mathrm{v}_0 = \frac{\mathrm{v_s}}{(1-\mathrm{v_s})} \end{aligned} \tag{20}$$

where E_s, v_s and H_s are Young's modulus, Poisson's ratio and depth of the foundation, respectively. In this paper, E_s is assumed to be temperature-dependent while v_s is assumed to be a constant. The governing electrodynamics Maxwell equations for a perfectly conducting and a plate subjected to a steady magnetic field, the exerted body force can be written as (Kolahchi *et al*. (2015), Ghorbanpour Arani and Zarei (2014), Ghorbanpour Arani *et al*. (2014)).

$$\vec{\mathrm{J}} = \nabla \times \vec{\mathrm{h}}\,, \qquad \vec{\mathrm{h}} = \nabla \times \left(\mathrm{D} \times \vec{\mathrm{H}}\right) \tag{21}$$

in which $\vec{J}$ is the current density, $\vec{h}$ is disturbing vectors of magnetic field, D is the displacement vector and $\vec{H} = (H_x\ ,\ 0\ ,\ 0)$ is magnetic field vector.

$$\begin{aligned} \vec{\mathrm{h}} = \nabla \times \left(\mathrm{D} \times \vec{\mathrm{H}}\right) = &-\vec{\mathrm{H}}_{\mathrm{x}}\left(\mathrm{V}_{,\mathrm{y}} + \mathrm{W}_{,\mathrm{z}}\right)\hat{\imath} + \vec{\mathrm{H}}_{\mathrm{x}}\left(\mathrm{V}_{,\mathrm{x}}\right)\hat{\jmath} \\ &+ \vec{\mathrm{H}}_{\mathrm{x}}\left(\mathrm{W}_{,\mathrm{x}}\right)\hat{\mathrm{k}} \end{aligned} \tag{22}$$

$$\begin{aligned} \vec{\mathrm{J}} = \nabla \times \vec{\mathrm{h}} = &\vec{\mathrm{H}}_{\mathrm{x}}\left(\mathrm{W}_{,\mathrm{xy}} - \mathrm{V}_{,\mathrm{xz}}\right)\hat{\imath} \\ &- \vec{\mathrm{H}}_{\mathrm{x}}\left(\mathrm{V}_{,\mathrm{yz}} + \mathrm{W}_{,\mathrm{zz}} + \mathrm{W}_{,\mathrm{xx}}\right)\hat{\jmath} \\ &+ \vec{\mathrm{H}}_{\mathrm{x}}\left(\mathrm{V}_{,\mathrm{xx}} + \mathrm{V}_{,\mathrm{yy}} + \mathrm{W}_{,\mathrm{zy}}\right)\hat{\mathrm{k}} \end{aligned} \tag{23}$$

Eq. (24) indicates the Lorentz force (f) in three directi ons (Reddy and Wang (2004)):

$$\begin{aligned} f &= f_x\hat{\imath} + f_y\hat{\jmath} + f_z\hat{k} \\ \vec{f} = \eta\left(\vec{J} \times \vec{H}\right) &= \eta\left[0\hat{\imath} + \vec{H}_x^2\left(V_{,xx} + V_{,yy} + W_{,yz}\right)\hat{\jmath}\right. \\ &\quad \left. + \vec{H}_x^2\left(V_{,yz} + W_{,zz} + W_{,xx}\right)\hat{k}\ \right] \end{aligned} \tag{24}$$

where η is the magnetic permeability; ∇ is the gradient operator. With substituting Eq. (6) into Eq. (24), therefore the Lorentz body force per unit volume of the plate can be obtained as

$$\begin{aligned} f_{mx} &= 0, \\ f_{my} &= \eta H_x^2\left[v_{,xx} + v_{,yy}\right], \\ f_{mz} &= \eta H_x^2\left[w_{,xx}\right]. \end{aligned} \tag{25}$$

Finally, the generated forces from the Lorentz force may be expressed as

$$F_m = \int_{-\frac{h}{2}}^{\frac{h}{2}} f_m\, dz = \begin{cases} F_{mx} = 0 \\ F_{my} = \eta h H_x^2\left[v_{,xx} + v_{,yy}\right] \\ F_{mz} = \eta h H_x^2\left[w_{,xx}\right] \end{cases} \tag{26}$$

3. Governing equation

The governing equations can be derived by Hamilton's principal as follows

$$\int_0^t \left(-\delta\Pi_s + \delta W_f\right)dt = 0 \tag{27}$$

Substituting Eqs. (16), (17), (18) and (26) into Eq. (27), integrating the resulting expression by parts and collecting t he coefficients of du, dv, dw and $d\phi$, the following diff erential equations can be obtained

$$\begin{aligned} \delta u:\ & N_{xx,x} + N_{xy,y} + F_{mx} = 0\,, \\ \delta v:\ & N_{xy,x} + N_{yy,y} + F_{my} = 0\,, \\ \delta w:\ & M_{xx,xx} + 2M_{xy,xy} + M_{yy,yy} + \left(N_{xx}w_{,x}\right)_{,x} \\ & + \left(N_{yy}w_{,y}\right)_{,y} + \left(N_{xy}w_{,x}\right)_{,y} \\ & + \left(N_{xy}w_{,y}\right)_{,x} + P + F_{mz} = 0\,, \\ \delta\phi:\ & \int_{-\frac{h}{2}}^{\frac{h}{2}} \left[\cos\left(\frac{\pi z}{h}\right)D_{x,x} + \cos\left(\frac{\pi z}{h}\right)D_{y,y}\right. \\ & \left. + \frac{\pi}{h}\sin\left(\frac{\pi z}{h}\right)D_z\right]dz = 0 \end{aligned} \tag{28}$$

Moment and stress resultants may be defined in terms of displacements following nonlinear strain–displacement relationships Eq. (7), stress–strain relationships Eq. (11) and stress resultants definitions Eq. (17) as

$$\begin{aligned} (1-\mu\nabla^2)M_{xx} &= -D_{11}\left(w_{,xx} + g\,w_{,txx}\right) \\ &\quad - D_{12}\left(w_{,yy} + g\,w_{,tyy}\right) + F_{31}\phi\,, \\ (1-\mu\nabla^2)M_{yy} &= -D_{12}\left(w_{,yy} + g\,w_{,tyy}\right) \\ &\quad - D_{22}\left(w_{,xx} + g\,w_{,txx}\right) + F_{31}\phi\,, \\ (1-\mu\nabla^2)M_{xy} &= -2D_{66}\left(w_{,xy} + g\,w_{,txy}\right), \\ (1-\mu\nabla^2)N_{xx} &= A_{11}\left(u_{,x} + \frac{1}{2}\left(w_{,x}\right)^2\right) \\ &\quad + A_{12}\left(v_{,y} + \frac{1}{2}\left(w_{,y}\right)^2\right) + 2e_{31}V_0 \\ &\quad - N_{xx}^T\,, \\ (1-\mu\nabla^2)N_{yy} &= A_{12}\left(u_{,x} + \frac{1}{2}\left(w_{,x}\right)^2\right) \\ &\quad + A_{22}\left(v_{,y} + \frac{1}{2}\left(w_{,y}\right)^2\right) + 2e_{31}V_0 \\ &\quad - N_{yy}^T\,, \\ (1-\mu\nabla^2)N_{xy} &= A_{66}\left(u_{,y}v_{,x} + w_{,x}w_{,y}\right). \end{aligned} \tag{29}$$

similarly, from Eqs. (12), we have

$$\begin{aligned} &\int_{-\frac{h}{2}}^{\frac{h}{2}} \left[\cos\left(\frac{\pi z}{h}\right)\left[D_{x,x} - \mu\nabla^2\left(D_{x,x}\right)\right]\right]dz = X_{11}\phi_{,xx}\,, \\ &\int_{-\frac{h}{2}}^{\frac{h}{2}} \left[\cos\left(\frac{\pi z}{h}\right)\left[D_{y,y} - \mu\nabla^2\left(D_{y,y}\right)\right]\right]dz = X_{11}\phi_{,yy}\,, \end{aligned} \tag{30}$$

$$\int_{-\frac{h}{2}}^{\frac{h}{2}}\left[\frac{\pi}{h}\sin\left(\frac{\pi z}{h}\right)[D_z-\mu\nabla^2 D_z]\right]dz = -F_{31}\left(w_{,xx}+w_{,yy}\right)-X_{33}\phi\,.$$

where $D_{11}=D_{22}$, $D_{12}=D_{21}$, $A_{11}=A_{22}$ and $A_{12}=A_{21}$ and also, we can define

$$\begin{Bmatrix}D_{11}\\D_{12}\\D_{66}\end{Bmatrix}=\frac{h^3}{12}\begin{Bmatrix}\tilde{c}_{11}\\\tilde{c}_{12}\\\tilde{c}_{66}\end{Bmatrix},\qquad \begin{Bmatrix}A_{11}\\A_{12}\\A_{66}\end{Bmatrix}=h\begin{Bmatrix}\tilde{c}_{11}\\\tilde{c}_{12}\\\tilde{c}_{66}\end{Bmatrix},\qquad \begin{Bmatrix}F_{31}\\X_{11}\\X_{33}\end{Bmatrix}=\begin{Bmatrix}\frac{2}{\pi}\tilde{e}_{31}h\\\frac{\tilde{\kappa}_{11}h}{2}\\\frac{\pi^2\tilde{\kappa}_{33}}{2h}\end{Bmatrix},\tag{31}$$

$$\begin{Bmatrix}N_{xx}^T\\N_{yy}^T\end{Bmatrix}=\int_{-\frac{h}{2}}^{\frac{h}{2}}\begin{Bmatrix}\tilde{\lambda}_{11}\\\tilde{\lambda}_{11}\end{Bmatrix}\Delta T\,dz$$

Here, D_{11} and D_{12} are the flexural rigidities of the PNP. D_{66} is called the torsional stiffness of the PNP. Assuming the density of plate material (ρ) as an even function of thickness (z) and applying the linear operator $(1-\mu\nabla^2)$ on each side of the equilibrium equations (28) and using relations of (29), (30) and Eq. (31), the following differential equations can be obtained

$$\begin{aligned}&A_{11}\left(u_{,xx}+\frac{1}{2}w_{,xx}w_{,x}\right)+A_{12}\left(v_{,xy}+\frac{1}{2}w_{,xy}w_{,y}\right)\\&+A_{66}\left(u_{,yy}+v_{,xy}+w_{,xy}w_{,y}\right.\\&\left.+w_{,yy}w_{,y}\right)+F_{mx}=0,\end{aligned}\tag{32}$$

$$\begin{aligned}&A_{12}\left(u_{,xy}+\frac{1}{2}w_{,xy}w_{,x}\right)+A_{22}\left(v_{,yy}+\frac{1}{2}w_{,yy}w_{,y}\right)\\&+A_{66}\left(u_{,xy}+v_{,xx}+w_{,xy}w_{,x}\right.\\&\left.+w_{,xx}w_{,y}\right)+F_{my}=0,\end{aligned}\tag{33}$$

$$\begin{aligned}&D_{11}\left(w_{,xxxx}+g\,w_{,txxxx}\right)\\&+2(D_{12}+2D_{66})\left(w_{,xxxx}\right.\\&\left.+g\,w_{,txxxx}\right)\\&+D_{22}\left(w_{,yyyy}+g\,w_{,tyyyy}\right)\\&+(1-\mu\nabla^2)(2e_{31}V_0)\left(w_{,xx}+w_{,yy}\right)\\&+(1-\mu\nabla^2)\left(-\tilde{\lambda}_{11}h\,\Delta T\right)\left(w_{,xx}\right.\\&\left.+w_{,yy}\right)\\&=(1-\mu\nabla^2)\left(k\,w\right.\\&-G_{\xi}\left(\cos^2\theta\;w_{,xx}\right.\\&\left.+2\cos\theta\sin\theta\;w_{,yx}+\sin^2\theta\;w_{,yy}\right)\\&-G_{\eta}\left(\sin^2\theta\;w_{,xx}\right.\\&\left.+2\sin\theta\cos\theta\;w_{,yx}+\cos^2\theta\;w_{,yy}\right)\\&\left.+F_{mz}\right)\\&+w_{,xx}\left[\frac{A_{11}}{2}\left(w_{,x}\right)^2+\frac{A_{12}}{2}\left(w_{,y}\right)^2\right]\\&+\left[A_{11}w_{,xx}w_{,x}+A_{12}w_{,xy}w_{,y}\right]w_{,x}\\&+w_{,yy}\left[\frac{A_{12}}{2}\left(w_{,x}\right)^2+\frac{A_{22}}{2}\left(w_{,y}\right)^2\right]\\&+\left[A_{12}w_{,xy}w_{,x}+A_{22}w_{,yy}w_{,y}\right]w_{,y}\\&+A_{66}w_{,xx}\left(w_{,y}\right)^2+4A_{66}w_{,x}w_{,xy}w_{,y}\\&+A_{66}w_{,yy}\left(w_{,x}\right)^2\\&+F_{31}\left(\phi_{,xx}+\phi_{,yy}\right),\end{aligned}$$

$$F_{31}\left(w_{,xx}+w_{,yy}\right)-X_{11}\left(\phi_{,xx}+\phi_{,yy}\right)+X_{33}\phi=0\,.\tag{35}$$

Based on Eqs. (32), (33), (34) and (35), the governing equations of nonlinear vibration for double viscoelastic nano plates can be expressed as,

$$\begin{aligned}&A_{11}\left(u_{i,xx}+\frac{1}{2}w_{i,xx}w_{i,x}\right)\\&+A_{12}\left(v_{i,xy}+\frac{1}{2}w_{i,xy}w_{i,y}\right)\\&+A_{66}\left(u_{i,yy}+v_{i,xy}+w_{i,xy}w_{i,y}\right.\\&\left.+w_{i,yy}w_{i,y}\right)+F_{mx}=0,\end{aligned}\tag{36}$$

$$\begin{aligned}&A_{12}\left(u_{i,xy}+\frac{1}{2}w_{i,xy}w_{i,x}\right)\\&+A_{22}\left(v_{i,yy}+\frac{1}{2}w_{i,yy}w_{i,y}\right)\\&+A_{66}\left(u_{i,xy}+v_{i,xx}+w_{i,xy}w_{i,x}\right.\\&\left.+w_{i,xx}w_{i,y}\right)+F_{my}=0,\end{aligned}\tag{37}$$

$$\begin{aligned}&D_{11}\left(w_{i,xxxx}+g\,w_{i,txxxx}\right)\\&+2(D_{12}+2D_{66})\left(w_{i,xxxx}\right.\\&\left.+g\,w_{i,txxxx}\right)\\&+D_{22}\left(w_{i,yyyy}+g\,w_{i,tyyyy}\right)\end{aligned}\tag{38}$$

$$
\begin{aligned}
&+(1-\mu\nabla^2)2e_{31}V_0\begin{pmatrix}w_{i,xx}\\+w_{i,yy}\end{pmatrix}\\
&\quad+(1-\mu\nabla^2)\left(-\tilde{\lambda}_{11}h\,\Delta T\right)\left(w_{i,xx}\right.\\
&\quad\left.+w_{i,yy}\right)\\
&=(1-\mu\nabla^2)\big(k\,w\\
&\quad-G_\xi\big(\cos^2\theta\;w_{,xx}\\
&\quad+2\cos\theta\sin\theta\;w_{,yx}\\
&\quad+\sin^2\theta\;w_{,yy}\big)\\
&\quad-G_\eta\big(\sin^2\theta\;w_{,xx}\\
&\quad+2\sin\theta\cos\theta\;w_{,yx}\\
&\quad+\cos^2\theta\;w_{,yy}\big)+F_{mz}\big)\\
&\quad+w_{i,xx}\left[\frac{A_{11}}{2}\left(w_{i,x}\right)^2\right.\\
&\quad\left.+\frac{A_{12}}{2}\left(w_{i,y}\right)^2\right]\\
&\quad+\left[A_{11}w_{i,xx}w_{i,x}\right.\\
&\quad\left.+A_{12}w_{i,xy}w_{i,y}\right]w_{i,x}\\
&\quad+w_{i,yy}\left[\frac{A_{12}}{2}\left(w_{i,x}\right)^2\right.\\
&\quad\left.+\frac{A_{22}}{2}\left(w_{i,y}\right)^2\right]\\
&\quad+\left[A_{12}w_{i,xy}w_{i,x}\right.\\
&\quad\left.+A_{22}w_{i,yy}w_{i,y}\right]w_{i,y}\\
&\quad+A_{66}w_{i,xx}\left(w_{i,y}\right)^2\\
&\quad+4A_{66}w_{i,x}w_{i,xy}w_{i,y}\\
&\quad+A_{66}w_{i,yy}\left(w_{i,x}\right)^2\\
&\quad+F_{31}\left(\phi_{i,xx}+\phi_{i,yy}\right),
\end{aligned}
$$

$$
F_{31}\left(w_{i,xx}+w_{i,yy}\right)-X_{11}\left(\phi_{i,xx}+\phi_{i,yy}\right)+X_{33}\phi_i=0\,. \tag{39}
$$

Subscript i $(i=1,2)$, for the variables of u,v,w and ϕ are employed to describe the upper and lower nanoplates, respectively. The following simply-supported boundary condition is considered in the present study

$$
\begin{cases}u=v=w=\phi=M_{xx}=0 & x=0,a\\ u=v=w=\phi=M_{yy}=0 & y=0,a\end{cases} \tag{40}
$$

4. GDQ method and solution procedure

The GDQ method is an efficient and accurate numerical approach in comparison with the weighted residual methods such as FE method (Zong and Zhang (2009)). In GDQ method a derivative of a function F is assumed as weighted linear sum of all functional values within the computational domain and at a given grid point (x_i,y_j), is approximated as

$$
\frac{d^nF}{dx^n}\Big|_{x=x_i}=\sum_{j=1}^{N}c_{ij}^{(n)}F(x_j) \tag{41}
$$

here

$$
C_{ij}^{(1)}=\frac{\pi(x_i)}{(x_i-x_j)\,\pi(x_j)}\qquad i,j=1,2,\dots,N,\quad i\neq j \tag{42}
$$

And $\pi(x_i)$ is defined as

$$
\pi(x_i)=\prod_{j=1}^{N}(x_i-x_j),\quad i\neq j \tag{43}
$$

And when $i=j$

$$
C_{ij}^{(1)}=c_{ii}^{(1)}=-\sum_{k=1}^{N}C_{ik}^{(1)},\qquad i=1,2,\dots,N,\quad i\neq k,\quad i=j \tag{44}
$$

the weighting coefficients for the second, third, and fourth derivatives are determined with using matrix multiplication

$$
\begin{aligned}
C_{ij}^{(2)}&=\sum_{k=1}^{N}C_{ik}^{(1)}C_{kj}^{(1)}\\
C_{ij}^{(3)}&=\sum_{k=1}^{N}C_{ik}^{(1)}C_{kj}^{(2)}=\sum_{k=1}^{N}C_{ik}^{(2)}C_{kj}^{(1)}\\
C_{ij}^{(4)}&=\sum_{k=1}^{N}C_{ik}^{(1)}C_{kj}^{(3)}=\sum_{k=1}^{N}C_{ik}^{(3)}C_{kj}^{(1)}\qquad i,j=1,2,\dots,N.
\end{aligned} \tag{45}
$$

using the following rule, the distribution of grid points based on Gauss-Chebyshev-Lobatto points in domain is calculated as

$$
\begin{aligned}
x_i&=\frac{a}{2}\left[1-\cos\left(\frac{i-1}{N-1}\pi\right)\right]\quad i=1,2,\dots,N,\\
y_j&=\frac{b}{2}\left[1-\cos\left(\frac{j-1}{M-1}\pi\right)\right]\quad j=1,2,\dots,M,
\end{aligned} \tag{46}
$$

to solve the time derivatives of Eqs. (36)-(39), we can assume it in the form

$$
\begin{aligned}
u(x,y,t)&=U(x,y)e^{\omega t}\\
v(x,y,t)&=V(x,y)e^{\omega t}\\
w(x,y,t)&=W(x,y)e^{\omega t}\\
\phi(x,y,t)&=\boldsymbol{\phi}(x,y)e^{\omega t}
\end{aligned} \tag{47}
$$

in which, ω is the complex eigenvalue. Finally, the governing equations (i.e. Eqs. (36) -(39)) can be expressed as

$$A_{11}\left(\sum_{k=1}^{N}\bar{C}_{i,k}^{(2)}U_{i_{k,j}}+\frac{1}{2}\left(\sum_{k=1}^{N}\bar{C}_{i,k}^{(2)}W_{i_{k,j}}\right)\left(\sum_{k=1}^{N}\bar{C}_{i,k}^{(1)}W_{i_{k,j}}\right)\circ W\right)+A_{12}\left(\begin{array}{c}\left(\sum_{k_1}^{N}\sum_{k_2}^{M}\bar{C}_{i,k_1}^{(1)}\bar{A}_{j,k_2}^{(1)}V_{i_{k_1,k_2}}\right)\\+\frac{1}{2}\left(\sum_{k_1}^{N}\sum_{k_2}^{M}\bar{C}_{i,k_1}^{(1)}\bar{A}_{j,k_2}^{(1)}W_{i_{k_1,k_2}}\right)\left(\sum_{k=1}^{N}\bar{A}_{i,k}^{(1)}W_{i_{k,j}}\right)\circ W\end{array}\right)$$
$$+A_{66}\left(\begin{array}{c}\sum_{k=1}^{M}\bar{A}_{j,k}^{(2)}U_{i_{i,k}}+\left(\sum_{k_1}^{N}\sum_{k_2}^{M}\bar{C}_{i,k_1}^{(1)}\bar{A}_{j,k_2}^{(1)}V_{i_{k_1,k_2}}\right)\\+\left(\sum_{k_1}^{N}\sum_{k_2}^{M}\bar{C}_{i,k_1}^{(1)}\bar{A}_{j,k_2}^{(1)}W_{i_{k_1,k_2}}\right)\left(\sum_{k=1}^{N}\bar{A}_{i,k}^{(1)}W_{i_{k,j}}\right)\circ W+\left(\sum_{k=1}^{M}\bar{A}_{j,k}^{(2)}W_{i_{i,k}}\right)\left(\sum_{k=1}^{N}\bar{A}_{i,k}^{(1)}W_{i_{k,j}}\right)\circ W\end{array}\right)=0, \tag{48}$$

$$A_{12}\left(\begin{array}{c}\left(\sum_{k_1}^{N}\sum_{k_2}^{M}\bar{C}_{i,k_1}^{(1)}\bar{A}_{j,k_2}^{(1)}U_{i_{k_1,k_2}}\right)\\+\frac{1}{2}\left(\sum_{k_1}^{N}\sum_{k_2}^{M}\bar{C}_{i,k_1}^{(1)}\bar{A}_{j,k_2}^{(1)}W_{i_{k_1,k_2}}\right)\left(\sum_{k=1}^{N}\bar{C}_{i,k}^{(1)}W_{i_{k,j}}\right)\circ W\end{array}\right)+A_{22}\left(\sum_{k=1}^{M}\bar{A}_{j,k}^{(2)}V_{i_{i,k}}+\frac{1}{2}\left(\sum_{k=1}^{M}\bar{A}_{j,k}^{(2)}W_{i_{i,k}}\right)\left(\sum_{k=1}^{M}\bar{A}_{j,k}^{(1)}W_{i_{i,k}}\right)\circ W\right)$$
$$+A_{66}\left(\begin{array}{c}\left(\sum_{k_1}^{N}\sum_{k_2}^{M}\bar{C}_{i,k_1}^{(1)}\bar{A}_{j,k_2}^{(1)}U_{i_{k_1,k_2}}\right)+\sum_{k=1}^{N}\bar{C}_{i,k}^{(2)}V_{i_{k,j}}\\+\left(\sum_{k_1}^{N}\sum_{k_2}^{M}\bar{C}_{i,k_1}^{(1)}\bar{A}_{j,k_2}^{(1)}W_{i_{k_1,k_2}}\right)\left(\sum_{k=1}^{N}\bar{C}_{i,k}^{(1)}W_{i_{k,j}}\right)\circ W+\left(\sum_{k=1}^{N}\bar{C}_{i,k}^{(2)}W_{i_{k,j}}\right)\left(\sum_{k=1}^{N}\bar{A}_{i,k}^{(1)}W_{i_{k,j}}\right)\circ W\end{array}\right)$$
$$+\eta hH_x^2\left(\sum_{k=1}^{N}\bar{C}_{i,k}^{(2)}V_{i_{k,j}}+\sum_{k=1}^{M}\bar{A}_{j,k}^{(2)}V_{i_{i,k}}\right)=0, \tag{49}$$

$$D_{11}\left(\sum_{k=1}^{N}\bar{C}_{i,k}^{(4)}W_{i_{k,j}}+g\omega\sum_{k=1}^{N}\bar{C}_{i,k}^{(4)}W_{i_{k,j}}\right)+2(D_{12}+2D_{22})\left(\sum_{k_1}^{N}\sum_{k_2}^{M}\bar{C}_{i,k_1}^{(2)}\bar{A}_{j,k_2}^{(2)}W_{i_{k_1,k_2}}+\right.$$
$$\left.+D_{22}\left(\sum_{k=1}^{M}\bar{A}_{j,k}^{(4)}W_{i_{i,k}}+g\omega\sum_{k=1}^{M}\bar{A}_{j,k}^{(4)}W_{i_{i,k}}\right)+(1-\mu\nabla^2)2e_{31}V_0\left(\sum_{k=1}^{N}\bar{C}_{i,k}^{(2)}W_{i_{k,j}}+\sum_{k=1}^{M}\bar{A}_{j,k}^{(2)}W_{i_{i,k}}\right)\right.$$
$$\left.+(1-\mu\nabla^2)\left(-\tilde{\lambda}_{11}h\,\Delta T\right)\left(\sum_{k=1}^{N}\bar{C}_{i,k}^{(2)}W_{i_{k,j}}+\sum_{k=1}^{M}\bar{A}_{j,k}^{(2)}W_{i_{i,k}}\right)\right.$$
$$=(1-\mu\nabla^2)\left(k\right.$$
$$-G_{\xi}\left(\cos^2\theta\left(\sum_{k=1}^{N}\bar{C}_{i,k}^{(2)}W_{i_{k,j}}\right)+2\cos\theta\sin\theta\left(\sum_{k_1}^{N}\sum_{k_2}^{M}\bar{C}_{i,k_1}^{(1)}\bar{A}_{j,k_2}^{(1)}W_{i_{k_1,k_2}}\right)\right.$$
$$\left.+\sin^2\theta\left(\sum_{k=1}^{M}\bar{A}_{j,k}^{(2)}W_{i_{i,k}}\right)\right)$$
$$-G_{\eta}\left(\sin^2\theta\left(\sum_{k=1}^{N}\bar{C}_{i,k}^{(2)}W_{i_{k,j}}\right)+2\sin\theta\cos\theta\left(\sum_{k_1}^{N}\sum_{k_2}^{M}\bar{C}_{i,k_1}^{(1)}\bar{A}_{j,k_2}^{(1)}W_{i_{k_1,k_2}}\right)\right.$$
$$\left.\left.+\cos^2\theta\left(\sum_{k=1}^{M}\bar{A}_{j,k}^{(2)}W_{i_{i,k}}\right)\right)+\eta hH_x^2\left(\sum_{k=1}^{N}\bar{C}_{i,k}^{(2)}W_{i_{k,j}}\right)\right)$$

$$
\begin{aligned}
&+\left[\left(\sum_{k=1}^{N}\bar{C}_{i,k}^{(2)}W_{i_{k,j}}\right)\left[\frac{A_{11}}{2}\left(\sum_{k=1}^{N}\bar{C}_{i,k}^{(1)}W_{i_{k,j}}\right)^{2}+\frac{A_{12}}{2}\left(\sum_{k=1}^{M}\bar{A}_{i,k}^{(1)}W_{i_{k,j}}\right)^{2}\right]\circ W\right.\\
&+\left(\sum_{k=1}^{N}\bar{C}_{i,k}^{(1)}W_{i_{k,j}}\right)\left[A_{11}\left(\sum_{k=1}^{N}\bar{C}_{i,k}^{(2)}W_{i_{k,j}}\right)\left(\sum_{k=1}^{N}\bar{C}_{i,k}^{(1)}W_{i_{k,j}}\right)\right.\\
&\left.+A_{12}\left(\sum_{k_1}^{N}\sum_{k_2}^{M}\bar{C}_{i,k_1}^{(1)}\bar{A}_{j,k_2}^{(1)}W_{i_{k_1,k_2}}\right)\left(\sum_{k=1}^{N}\bar{A}_{i,k}^{(1)}W_{i_{k,j}}\right)\right]\circ W\\
&+\left(\sum_{k=1}^{M}\bar{A}_{i,k}^{(2)}W_{i_{k,j}}\right)\left[\frac{A_{12}}{2}\left(\sum_{k=1}^{N}\bar{C}_{i,k}^{(1)}W_{i_{k,j}}\right)^{2}+\frac{A_{22}}{2}\left(\sum_{k=1}^{M}\bar{A}_{i,k}^{(1)}W_{i_{k,j}}\right)^{2}\right]\circ W\\
&+\left(\sum_{k=1}^{N}\bar{A}_{i,k}^{(1)}W_{i_{k,j}}\right)\left[A_{12}\left(\sum_{k_1}^{N}\sum_{k_2}^{M}\bar{C}_{i,k_1}^{(1)}\bar{A}_{j,k_2}^{(1)}i_{k_1,k_2}\right)\left(\sum_{k=1}^{N}\bar{C}_{i,k}^{(1)}W_{i_{k,j}}\right)\right.\\
&\left.+A_{22}\left(\sum_{k=1}^{N}\bar{A}_{i,k}^{(2)}W_{i_{k,j}}\right)\left(\sum_{k=1}^{N}\bar{A}_{i,k}^{(1)}W_{i_{k,j}}\right)\right]\circ W+A_{66}\left(\left(\sum_{k=1}^{N}\bar{C}_{i,k}^{(2)}W_{i_{k,j}}\right)\left(\sum_{k=1}^{M}\bar{A}_{i,k}^{(1)}W_{i_{k,j}}\right)^{2}\right)\circ W\\
&+4A_{66}\left(\left(\sum_{k=1}^{N}\bar{C}_{i,k}^{(1)}W_{i_{k,j}}\right)\left(\sum_{k_1}^{N}\sum_{k_2}^{M}\bar{C}_{i,k_1}^{(1)}\bar{A}_{j,k_2}^{(1)}W_{i_{k_1,k_2}}\right)\left(\sum_{k=1}^{N}\bar{A}_{i,k}^{(1)}W_{i_{k,j}}\right)\right)\circ W\\
&\left.+A_{66}\left(\left(\sum_{k=1}^{N}\bar{A}_{i,k}^{(2)}W_{i_{k,j}}\right)\left(\sum_{k=1}^{M}\bar{C}_{i,k}^{(1)}W_{i_{k,j}}\right)^{2}\right)\circ W\right]+F_{31}\left(\sum_{k=1}^{N}\bar{C}_{i,k}^{(2)}\boldsymbol{\phi}_{i_{k,j}}+\sum_{k=1}^{M}\bar{A}_{j,k}^{(2)}\boldsymbol{\phi}_{i_{i,k}}\right),
\end{aligned}
\tag{50}
$$

$$
\begin{aligned}
&F_{31}\left(\sum_{k=1}^{N}\bar{C}_{i,k}^{(2)}W_{i_{k,j}}+\sum_{k=1}^{M}\bar{A}_{j,k}^{(2)}W_{i_{i,k}}\right)\\
&\quad-X_{11}\left(\sum_{k=1}^{N}\bar{C}_{i,k}^{(2)}\boldsymbol{\phi}_{i_{k,j}}\right.\\
&\quad\left.+\sum_{k=1}^{M}\bar{A}_{j,k}^{(2)}\boldsymbol{\phi}_{i_{i,k}}\right)+X_{33}\boldsymbol{\phi}_1=0.
\end{aligned}
\tag{51}
$$

In Eqs. (48)-(51), $\bar{C}$ and $\bar{A}$ denote the weighting coefficients in x and y directions, respectively. In order to analyses the nonlinear matrix, we can use two mathematical products (Hadamard and Kronecker) (Chen *et al*. (2000), Lancaster and Timenetsky (1985)). Eqs. (48)-(51), can be explained in matrix form which is called nonlinear eigenvalue problem.

$$
(\omega[D]+[K_L+K_{NL}])\begin{Bmatrix}U_1\\V_1\\W_1\\\boldsymbol{\phi}_1\\U_2\\V_2\\W_2\\\boldsymbol{\phi}_2\end{Bmatrix}=0,
\tag{52}
$$

where D, K_L and K_{NL} are damping matrix, the linear stiffness matrix and the nonlinear stiffness matrix which are a functions of U,V,W and $\boldsymbol{\phi}$. The stiffness matrices in Eqs. (52) can be expressed as

$$
[D]=\begin{bmatrix}
[0] & [0] & [0] & [0] & [0] & [0] & [0] & [0]\\
[0] & [0] & [0] & [0] & [0] & [0] & [0] & [0]\\
[0] & [0] & [D_{3w}^{3}] & [0] & [0] & [0] & [0] & [0]\\
[0] & [0] & [0] & [0] & [0] & [0] & [0] & [0]\\
[0] & [0] & [0] & [0] & [0] & [0] & [0] & [0]\\
[0] & [0] & [0] & [0] & [0] & [0] & [0] & [0]\\
[0] & [0] & [0] & [0] & [0] & [0] & [D_{7w}^{7}] & [0]\\
[0] & [0] & [0] & [0] & [0] & [0] & [0] & [0]
\end{bmatrix},
$$

$$
[K_L]=\begin{bmatrix}
[K_{L_{1u}}^{1}] & [K_{L_{1v}}^{2}] & [0] & [0] & [0] & [0] & [0] & [0]\\
[K_{L_{2u}}^{1}] & [K_{L_{2v}}^{2}] & [0] & [0] & [0] & [0] & [0] & [0]\\
[0] & [0] & [K_{L_{3w}}^{3}] & [K_{L_{3\phi}}^{4}] & [0] & [0] & [K_{L_{7w}}^{3}] & [0]\\
[0] & [0] & [K_{L_{4w}}^{3}] & [K_{L_{4\phi}}^{4}] & [0] & [0] & [0] & [0]\\
[0] & [0] & [0] & [0] & [K_{L_{5u}}^{5}] & [K_{L_{5v}}^{6}] & [0] & [0]\\
[0] & [0] & [0] & [0] & [K_{L_{6u}}^{5}] & [K_{L_{6v}}^{6}] & [0] & [0]\\
[0] & [0] & [K_{L_{7w}}^{3}] & [0] & [0] & [0] & [K_{L_{7w}}^{7}] & [K_{L_{7\phi}}^{8}]\\
[0] & [0] & [0] & [0] & [0] & [0] & [K_{L_{8w}}^{7}] & [K_{L_{8\phi}}^{8}]
\end{bmatrix}
$$

$$
[K_{NL}]=\begin{bmatrix}
[0] & [0] & [K_{NL_{1w}}^{3}] & [0] & [0] & [0] & [0] & [0]\\
[0] & [0] & [K_{NL_{2w}}^{3}] & [0] & [0] & [0] & [0] & [0]\\
[0] & [0] & [K_{NL_{3w}}^{3}] & [0] & [0] & [0] & [0] & [0]\\
[0] & [0] & [0] & [0] & [0] & [0] & [K_{NL_{5w}}^{7}] & [0]\\
[0] & [0] & [0] & [0] & [0] & [0] & [K_{NL_{6w}}^{7}] & [0]\\
[0] & [0] & [0] & [0] & [0] & [0] & [K_{NL_{7w}}^{7}] & [0]\\
[0] & [0] & [0] & [0] & [0] & [0] & [0] & [0]
\end{bmatrix}.
\tag{53}
$$

This nonlinear equation can be solved using a direct iterative process as follows (Arani (2013)): First, term of nonlinearity is ignored by taking $K_{NL}=0$ to obtain the eigenvalue problem demonstrated in Eq. (52). This yields the linear eigenvalue ω_L and corresponding eigenvector (U,V,W,ϕ). Using linear corresponding eigenvector

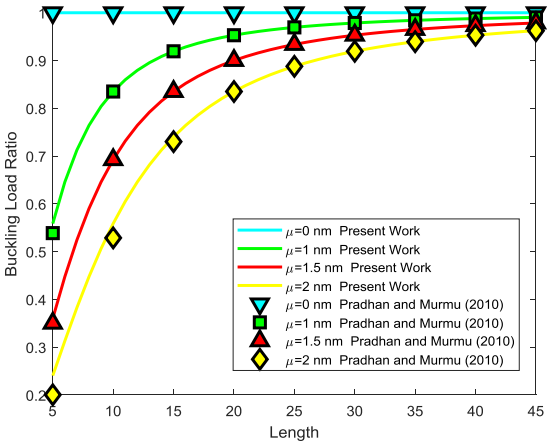

Fig. 2 Variation of buckling load ratio with the length of a square nanoplate for various nonlocal parameters

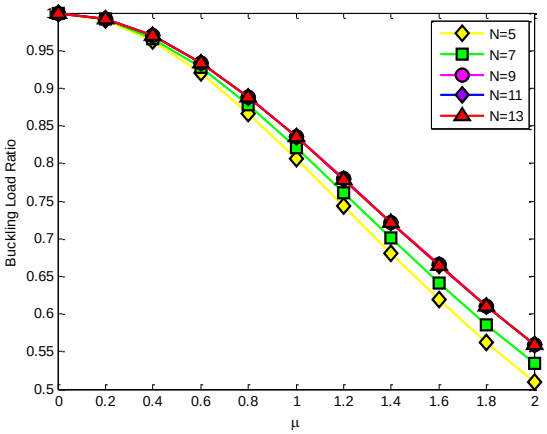

Fig. 3 Convergence behavior of buckling ratio against number of grid point of GDQ method

(U, V, W, ϕ), K_{NL} could be calculated. Then by substituting K_{NL} into Eq. (52), eigenvalue problem is solved. This would give the nonlinear eigenvalue ω_{NL} and the new eigenvector. The above process is repeated iteratively until the frequency values from the two subsequent iterations 'r' and '$r+1$' satisfy the prescribed convergence criteria as

$$\frac{||\omega_{NL}|^{r+1} - |\omega_{NL}|^{r}|}{|\omega_{NL}|^{r}} < \varepsilon_0 \tag{54}$$

where ε_0 is a small value number and in this present ε_0 is 10^{-4}.

5. Results and discussion

Firstly, the results are compared with the available literatures to verify the accuracy of the present formulations. Since the present results are the first reported results for the double viscoelastic nanoplates, no available results may be found in literature to be used for comparison purposes. For this reason, present results are verified by results of the single layered nanoplate. The values obtained by the local and nonlocal models are shown in Fig. 2. The present results in Fig. 2 are in a good agreement with Pradhan and Murmu (2010).

Fig. 2 describes the effects of small scale, that buckling ratio is defined as the ratio of the nonlocal buckling load to the local buckling load. The elastic modulus $= 1.06\ Tpa$, length or breadth $L = 10\ nm$, thickness of each plate $h = 0.34\ nm$, the Poisson's ratio $\nu = 0.3$ and density $\rho = 2250\ kg/m^3$ are employed. Characteristics and properties of material are taken from Pradhan and Murmu (2010). It's noted that, in Fig. 2, we compared the results of the buckling load ratio of isotropic square plate with simply supported boundary conditions with the available literatures. These results also are obtained without considering the nonlinear terms, effects of elastic medium in governing equation. In evaluating the nonlinear buckling ratio of the nano plate, we need to obtain the minimum number of grid points that makes the convergence. The convergence and accuracy of the GDQ method based on the number of grid points is plotted in Fig. 3 and Table 1 for simple support in all sides. For illustration of small scale or nonlocal effects, the maximum length of the SLGS is taken as 45.2896 nm. This maximum value is also used by Pradhan and Murmu (2010) for the side length of the graphene sheet. The scale coefficients were taken as $\mu = 0.0, 1.0, 1.5$ and $2.0\ nm$

Table 1 Comparison of the convergence behavior of buckling ratio against number of grid point of GDQ method

N / μ	5×5	7×7	9×9	11×11	13×13
0.4	0.9630	0.9662	0.9695	0.9694	0.9694
1	0.8065	0.8208	0.8358	0.8351	0.8351
1.6	0.6194	0.6415	0.6653	0.6643	0.6643
2	0.5102	0.5338	0.5599	0.5588	0.5588

As basic issues in a numerical analysis, the convergence characteristics and accuracy of the GDQ solution should be carefully assessed. Table 1 demonstrates the convergence and accuracy of the GDQ method based on the number of grid points in evaluating the nonlinear buckling load ratio of isotropic square plate with simply supported boundary conditions. Fast rate of convergence of the method are quite evident and it is found that thirteen DQ grid points can yield accurate results.

Nonlinear buckling of double viscoelastic nanoplates

In this section, we will present the semi-analytical study on the nonlinear buckling load ratio of the double viscoelastic nanoplate with all edges simply supported. Assume that the nanoplate is made of PZT-4 with the material properties listed in Table 2 (Ke and Wang (2012), Wang (2002), Liu *et al*. (2013)). In Table 3, the nonlinear buckling ratio of the viscoelastic double nanoplate evaluated accounting for nonlocal parameters ($\mu = 0.2, 0.5, 1\ nm$) and the aspect ratio ($\beta = 1/4, 1/2, 1, 3/2$).

Table 2 Material properties of PZT-4 (Ke and Wang (2012), Wang (2002), Chen *et al*. (2013))

$c_{11}\,(Gpa)$	$c_{12}\,(Gpa)$	$c_{13}\,(Gpa)$	$c_{33}\,(Gpa)$	$c_{66}\,(Gpa)$	$e_{31}(C/m^2)$	$e_{15}(C/m^2)$	$e_{33}(C/m^2)$
132	71	73	115	30.5	-4.1	10.5	14.1
$k_{11}(C/V\,m)$	$k_{33}(C/V\,m)$	$\lambda_{11}(N/m^2\,k)$	$\lambda_{33}(N/m^2\,k)$	$p_1(C/m^2\,k)$	$p_3(C/m^2\,k)$	$\rho\,(kg/m^3)$	
5.841×10^{-9}	7.124×10^{-9}	4.738×10^{-5}	4.529×10^{-5}	0.25×10^{-4}	0.25×10^{-4}	7500	

Table 3 nonlinear buckling ratio for various values of β, μ, G_η, and V_0 against maximum transverse amplitude $(w_{1\,max}=1)$, the viscoelastic damping coefficient $(g=0.01)$ and $\left(H_x=0,\ \theta=45°,\ G_\xi=4.14,\ \Delta T=0\right)$

		$G_\eta=0$				$G_\eta=4.14$			
		V_0							
μ	β	0	0.25	0.5	0.75	0	0.25	0.5	0.75
0.2	1/4	42.2749	50.5252	54.6911	57.3192	44.3959	51.4857	55.2610	57.7120
	1/2	40.8243	49.0448	53.3348	56.0621	41.0188	49.1346	53.3880	56.0984
	1	34.8322	45.2625	50.5014	53.7317	36.4306	45.9799	50.9165	54.0087
	3/2	29.0875	42.5617	48.8274	52.5310	35.3037	45.2099	50.3185	53.5084
0.5	0.5	56.7526	60.9863	45.5285	31.2984	57.7718	61.5436	42.3626	29.2652
	1	56.0736	60.1615	53.2031	37.9819	56.1639	60.2104	52.8989	37.7853
	1.5	53.3771	58.1990	60.9726	50.9388	54.0827	58.5582	61.2110	49.3671
	2	50.8964	56.8885	60.0434	57.8300	53.5844	58.1729	60.8687	52.2119
1	0.5	48.6285	23.1831	10.6822	3.1366	42.0466	20.2652	9.0147	2.0472
	1	53.1387	27.7072	14.7012	6.6971	52.5337	27.4322	14.5425	6.5928
	1.5	60.7713	39.3630	23.2558	13.5187	61.2536	37.1443	21.9926	12.6963
	2	59.1566	47.7373	28.3740	17.1099	60.9118	39.5256	23.8131	14.1839

Table 4 nonlinear buckling ratio for various values of H_x, μ, V_0, and ΔT against maximum transverse amplitude $(w_{1\,max}=1)$, the viscoelastic damping coefficient $(g=0.01)$ and $\left(\beta=1,\ \theta=45°,\ G_\xi=4.14,\ \mathrm{G}_\eta=4.14\right)$

		$\Delta T=0\,K$				$\Delta T=100\,K$			
		H_x							
μ	V_0	0	0. 5	1	1.5	0	0. 5	1	1.5
0.2	0	9.5394	15.3384	20.0371	23.9225	15.8734	4.0757	4.7076	11.5027
	0.25	36.6747	38.2776	39.7123	41.0044	31.2571	33.4976	35.4617	37.1982
	0.5	46.0919	46.8441	47.5430	48.1942	43.7516	44.6838	45.5418	46.3344
	0.75	50.9820	51.4274	51.8496	52.2506	49.6530	50.1724	50.6620	51.1246
0.5	0	42.7768	45.1555	47.0972	48.7165	32.4718	37.2394	40.8056	43.5803
	0.25	54.1912	54.9093	55.5613	56.1572	51.8247	52.7938	53.6540	54.4246
	0.5	58.6147	58.9982	59.3605	59.7038	57.4586	57.9130	58.3382	58.7376
	0.75	61.2490	61.5092	61.7599	59.4558	60.4957	60.7861	61.0645	61.3318
1	0	54.4161	55.7471	56.8628	57.8194	48.9091	51.4194	53.3359	54.8620
	0.25	61.3288	61.0701	56.6001	52.5783	59.7475	60.3809	60.9592	61.4916
	0.5	36.7982	34.4760	32.3220	30.3182	44.0439	41.1545	38.4989	36.0492
	0.75	21.7934	20.4418	19.1640	17.9540	25.8453	24.2587	22.7666	21.3604

In the present investigation for various values of $(g=0.01)$ and the elastomeric coefficients $\left(G_\eta=0,\ 4.14\right)$, nonlinear buckling load ratio, are listed. Results show that by increasing the electric voltage from 0 to 0.75, the buckling loads for small nonlocal parameter $(\mu=0.1\,nm)$ increase but for higher nonlocal parameter $(\mu=0.5,1\,nm)$ reduce in both the elastomeric coefficients $\left(G_\eta=0,\ 4.14\right)$. The same trend has been observed for the elastomeric coefficient $\left(G_\eta=4.14\right)$. To better evaluate, let us define the following non-dimensional variable for the Lorentz force coefficient

$$H_x=\sqrt{\frac{\eta\,H_x^2}{EA}} \tag{55}$$

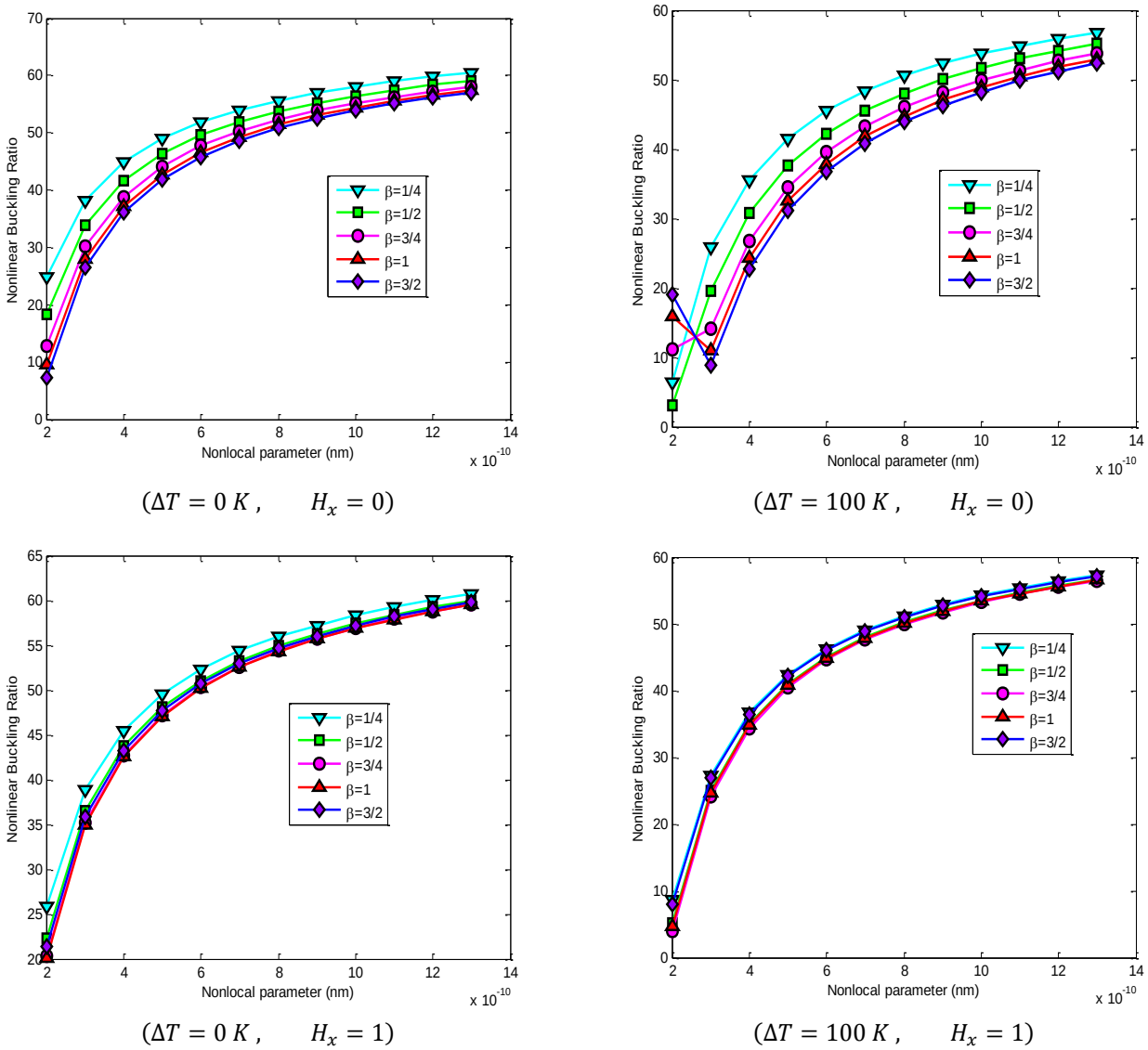

$(\Delta T = 0\ K\ ,\quad H_x = 0)$ $(\Delta T = 100\ K\ ,\quad H_x = 0)$

$(\Delta T = 0\ K\ ,\quad H_x = 1)$ $(\Delta T = 100\ K\ ,\quad H_x = 1)$

Fig. 4 nonlinear buckling ratio for various values of (β) against nonlocal parameter μ, electric voltage $(V_0 = 0)$ for variation of temperature $(\Delta T = 0\ K,\ 100\ K)$, coefficient of dimensionless magnetic field $(H_x = 0, 1)$, maximum transverse amplitude $(w_{1\,max} = 1)$ and the viscoelastic damping coefficient $(g = 0.01)$

Small scale effects on nonlinear buckling of nanoplates

To understand the effects of the small-scale coefficients (nonlocal parameter) on the double piezo nanoplates, numerical nonlinear buckling load results with considering the viscoelastic damping coefficient (g), for different values of nonlocal parameter (μ) are obtained. Furthermore, are also considered effects of temperature variations, (ΔT) and magnetic field. Figs. 4 demonstrate the effects of the small-scale coefficients in nonlinear buckling behavior for various aspect ratios. Based on the obtained results, it can be concluded that the small scale effect makes the nanoplate more flexible (Fig. 10) as the nonlocal model may be viewed as atoms linked by elastic springs while the local continuum model assumes the spring constant to take on an infinite value (Jomehzadeh and Saidi (2011)).

Electric voltage effects on nonlinear buckling of nanoplates

The effects of magnetic field (H_x) and external electric voltage (V_0) on the nonlinear buckling ratio of a double-piezo viscoelastic nanoplate are described in Figs. 5 and 6. It is seen that first the buckling load increase nonlinearly with increasing electric voltage and then decrease nonlinearly. The results are extracted for various nonlocal parameters $(\mu = 0.5, 1\ nm)$, variation of temperature $(\Delta T = 0,\ 100\ K)$ for simply supported boundary conditions. Results obtained in Figs. 5 and 6 reveals that by increasing electric voltage in high nonlocal parameter $(\mu = 1\ nm)$, the nonlinear buckling ratio decreases. I.e. the small scale (nonlocal parameter) effect makes the nanoplate more flexible, but in low nonlocal parameters $(\mu = 0.5\ nm)$, it is inverses.

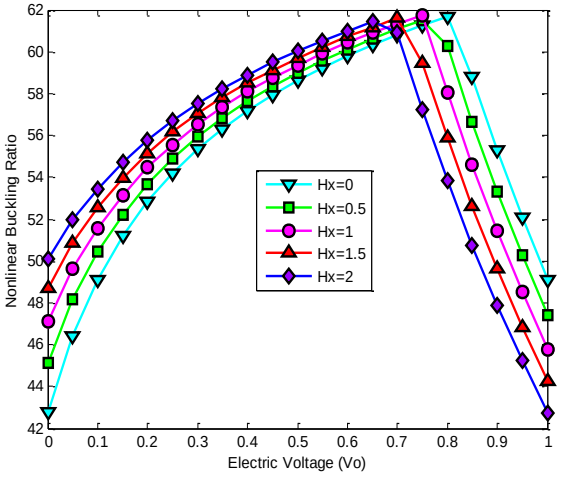

$(\Delta T = 0\ K\ ,\quad \mu = 0.5\ nm)$

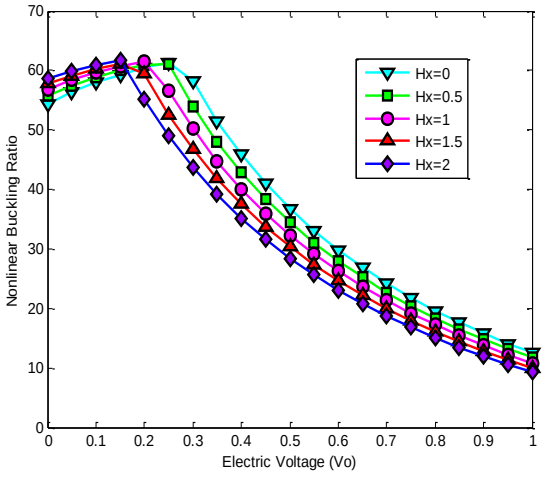

$(\Delta T = 0\ K\ ,\quad \mu = 1\ nm)$

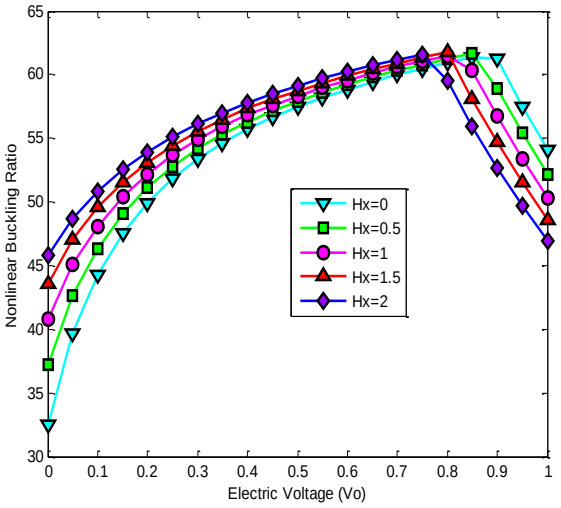

$(\Delta T = 100\ K\ ,\quad \mu = 0.5\ nm)$

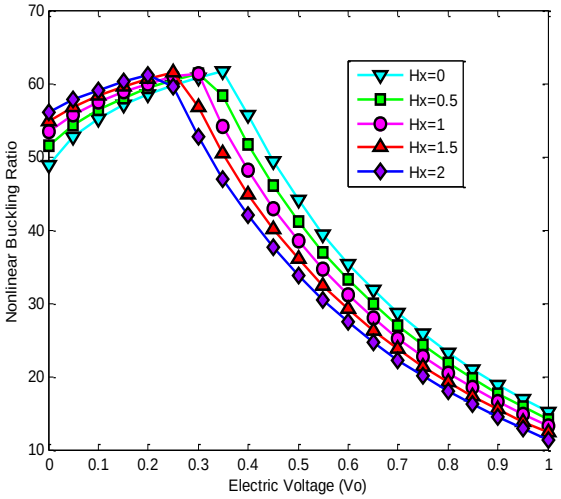

$(\Delta T = 100\ K\ ,\quad \mu = 1\ nm)$

Fig. 5 nonlinear buckling ratio for various values of (H_x) against electric voltage (V_0) for variation of temperature $(\Delta T = 0\ K,\ 100\ K)$, nonlocal parameter $(\mu = 0.5\ nm\ , 1\ nm)$, maximum transverse amplitude $(w_{1\ max} = 1)$ and the viscoelastic damping coefficient $(g = 0.01)$

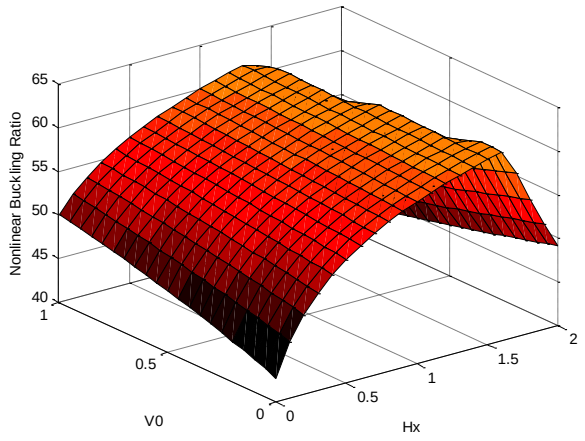

$(\Delta T = 0\ K\ ,\quad \mu = 0.5\ nm)$

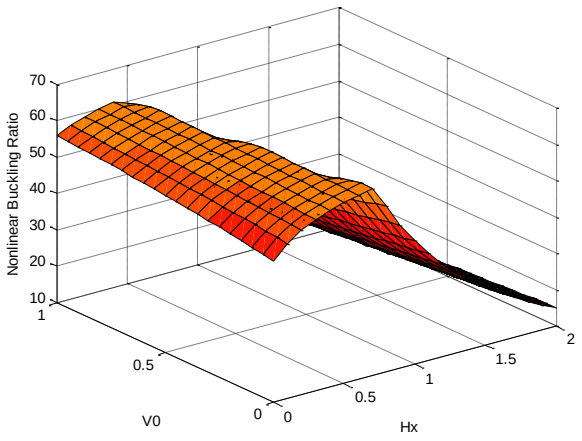

$(\Delta T = 100\ K\ ,\quad \mu = 1\ nm)$

Fig. 6 nonlinear buckling ratio for various values of (H_x) and electric voltage (V_0) for variation of temperature $(\Delta T = 0\ K,\ 100\ K)$, nonlocal parameter $(\mu = 0.5\ nm\ , 1\ nm)$, maximum transverse amplitude $(w_{1\ max} = 1)$ and the viscoelastic damping coefficient $(g = 0.01)$.

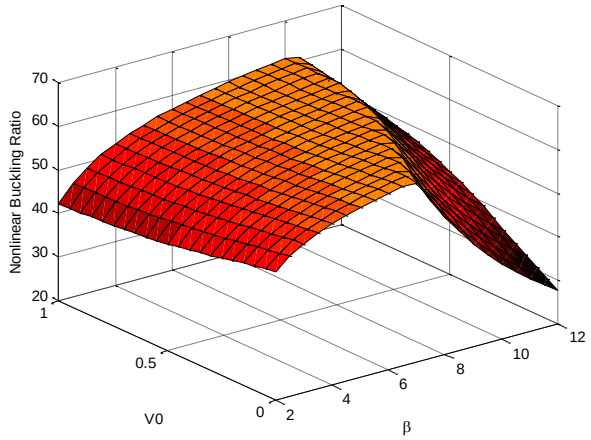

$(\Delta T = 0\ K\ ,\quad \mu = 0.5\ nm)$

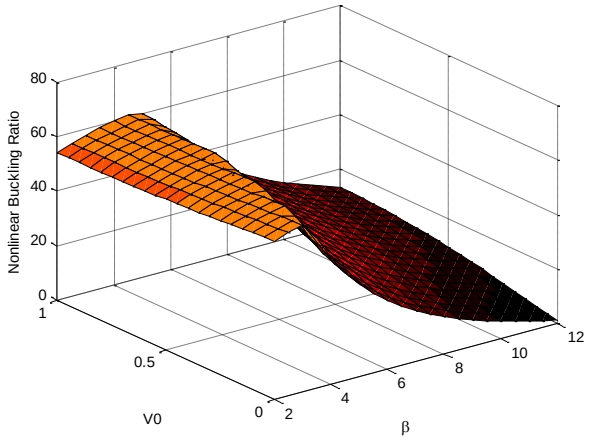

$(\Delta T = 0\ K\ ,\quad \mu = 1\ nm)$

Fig. 7 nonlinear buckling ratio for various values of β and electric voltage (V_0) for nonlocal parameter $(\mu = 0.5, 1\ nm)$, variation of temperature $(\Delta T = 0\ K)$, maximum transverse amplitude $(w_{1\ max} = 1)$ and the viscoelastic damping coefficient $(g = 0.01)$

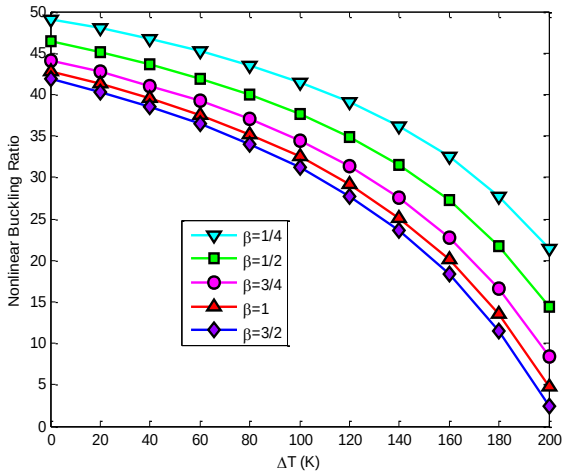

$(H_x = 0\ ,\quad \mu = 0.5\ nm)$

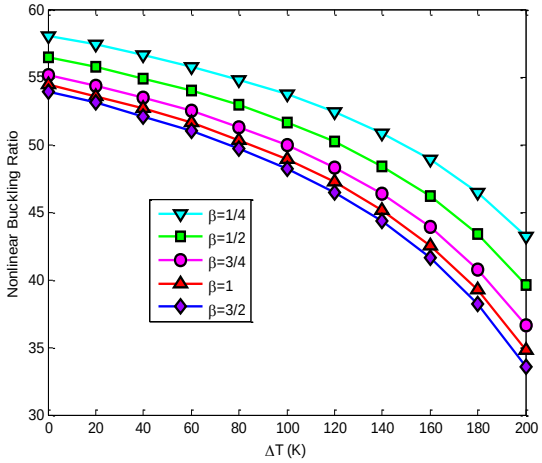

$(H_x = 0\ ,\quad \mu = 1\ nm)$

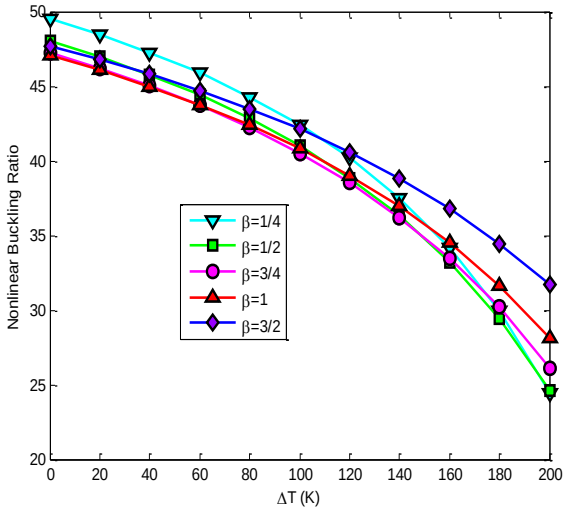

$(H_x = 1\ ,\quad \mu = 0.5\ nm)$

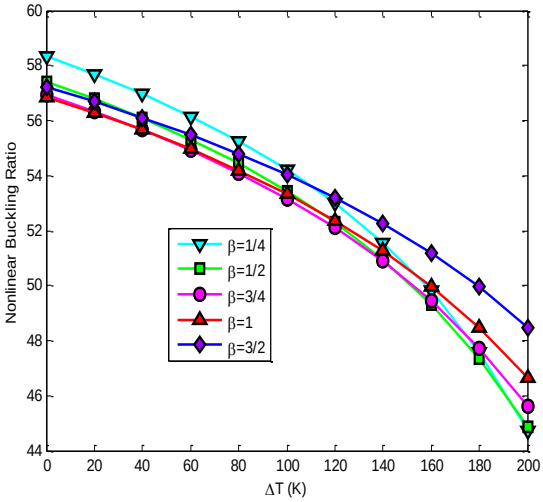

$(H_x = 1\ ,\quad \mu = 1\ nm)$

Fig. 8 nonlinear buckling ratio for various values of (β) against temperature (ΔT) and variation of coefficient of dimensionless magnetic field $(H_x = 0, 1)$, nonlocal parameter $(\mu = 0.5\ nm\ , 1\ nm)$, maximum transverse amplitude $(w_{1\ max} = 1)$ and the viscoelastic damping coefficient $(g = 0.01)$

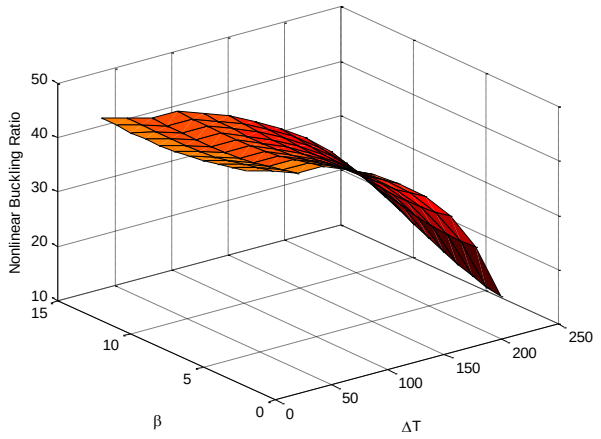

$(H_x = 1\,,\quad \mu = 0.5\ nm)$

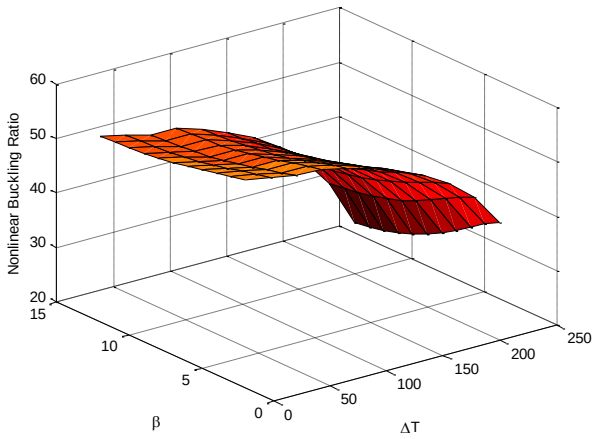

$(H_x = 0\,,\quad \mu = 1\ nm)$

Fig. 9 nonlinear buckling ratio for various values of (β) and variation of temperature (ΔT) and coefficient of dimensionless magnetic field $(H_x = 0, 1)$, nonlocal parameter $(\mu = 0.5\ nm\,, 1\ nm)$, maximum transverse amplitude $(w_{1\ max} = 1)$ and the viscoelastic damping coefficient $(g = 0.01)$

Fig. 7 shows the effects of aspect ratio (β) or width to length ratio (b/a) on the nonlinear buckling ratio of a double-piezo nanoplate against increasing electric voltage (V_0). The results are extracted for various nonlocal parameters $(\mu = 0.5, 1\ nm)$, variation of temperature $(\Delta T = 0, 100\ K)$ for simply supported boundary conditions, respectively. From Figs. 5, 6 and 7, it can be found that electric voltage can decline the stiffness of the structure. Fig. 14 shows the nonlinear buckling behavior for different values of the viscoelastic damping coefficient of the nanoplates versus electric voltage with nonlocal parameters $(\mu = 1\ nm)$ and temperature fields $(\Delta T = 100\ K)$. From this figure, it can be seen that the electric voltage has the more effect on the buckling behavior while the effect of viscoelastic coefficient is little and by increase viscoelastic coefficient, nonlinear buckling load ratio almost remains unchanged.

Thermal effects on nonlinear buckling of nanoplates

To illustrate the effect of temperature on the nonlinear buckling ratio, in this section, the effects of uniform temperature fields on the nonlinear buckling ratio versus increasing aspect ratio (β) and nonlocal parameters (μ) are shown Figs. 8-11. This is obvious that increasing the temperature (ΔT), the nonlinear buckling ratio decreases in all of plots. Fig. 10 illustrates the variation of the nonlinear buckling ratio versus increasing of uniform temperature field $(0 - 200\ K)$ for different nonlocal parameters. It is revealed that for each temperature field, with increasing nonlocal parameter, nonlinear buckling ratio can increases or decreases that depends values of electric voltage and magnetic field. It is also revealed that the nonlinear buckling ratio increases in absence electric voltage $(V_0 = 0)$.

Magnetic field effects on nonlinear buckling of nanoplates

Applying magnetic field in axial direction generate the force in radial direction that is called Lorentz force. The effect of magnetic field on nonlinear buckling behavior of double-piezo nanoplate is shown in Figs. 6. It is concluded that nonlinear buckling ratio can decreases with increasing magnetic intensity or can increases with increasing magnetic intensity (Figs. 5, 6 and 10). In absence electric voltage $(V_0 = 0)$ with increasing magnetic intensity, the nonlinear buckling ratio increases. It is evident that the magnetic field is fundamentally an effective factor on increasing or decreasing buckling load of system.

Elastomeric foundation effects on nonlinear buckling of nanoplates

Fig. 12 describes nonlinear buckling behavior versus increasing electric voltage (V_0) for the effect of elastomeric foundation coefficient $(G_\xi = 0,\ 4.14)$ and nonlocal parameters $(\mu = 0.8, 1\ nm)$. It can be found that the effect of elastomeric medium on buckling behavior is more significant than temperature and magnetic field.
The elastomeric medium is made of Poly dimethylsiloxane (PDMS) which the temperature-dependent material properties in which $(T = T_0 + \Delta T)$ and $(T_0 = 300\ K)$ (room temperature). It's noted that, in the present, $(E_s = (3.22 - 0.0034T)Gpa,\ \upsilon_s = 0.48\,,)$ are taken from Refs. (Kolahchi (2015), Shen (2009), Kutlu and Omurtag (2012)). The Winkler coefficient (k) PDMS coefficients $(G_\xi = 0, 4.14\,,\ G_\eta = 0,\ 4.14\,,\ \theta = 45^\circ)$ for the elastomeric foundation are also taken similar values of modulus coefficients were taken by Refs. (Kolahchi (2015), Shen (2009), Kutlu and Omurtag (2012)).

6. Conclusions

In the present research, the nonlinear thermo-electro-elastic buckling behavior of viscoelastic nanoplates is investigated based on nonlocal elasticity theory. Employing nonlinear strain-displacement relations, the geometrical nonlinearity is modeled while governing equations are

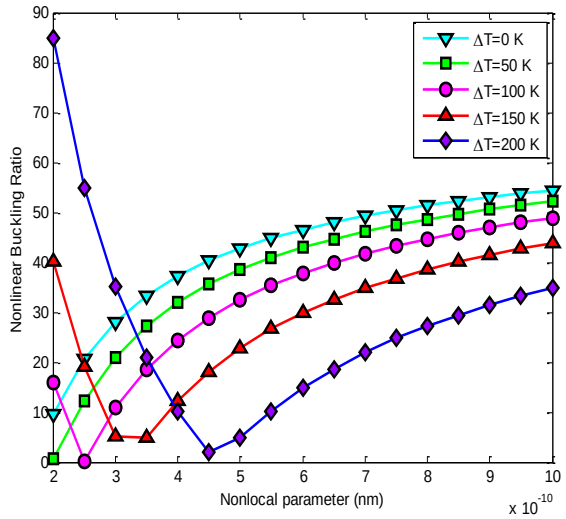

$(V_0 = 0\,, \quad H_x = 0)$

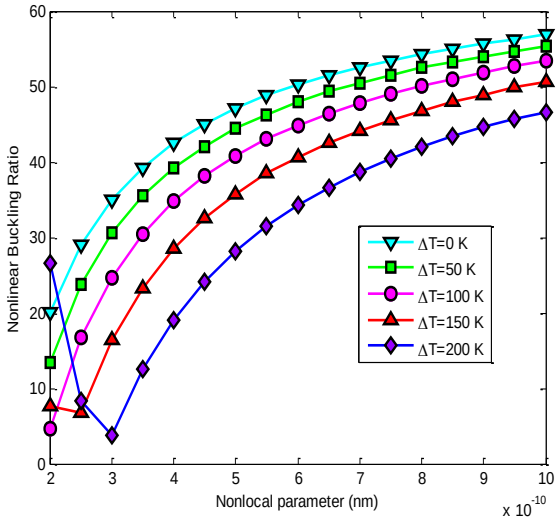

$(V_0 = 0\,, \quad H_x = 1)$

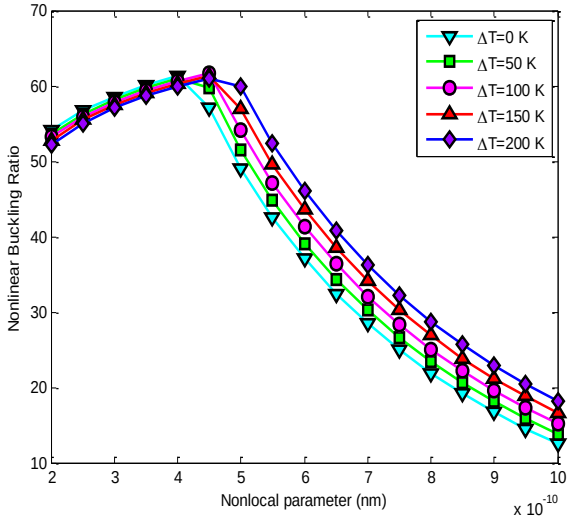

$(V_0 = 1\,, \quad H_x = 0)$

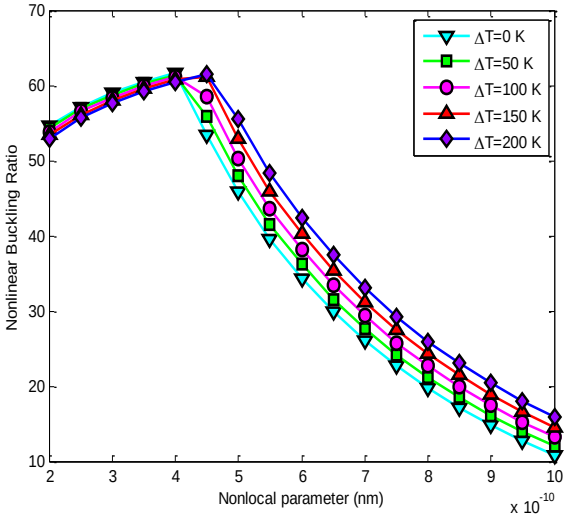

$(V_0 = 1\,, \quad H_x = 1)$

Fig. 10 nonlinear buckling ratio for various values of (ΔT) against nonlocal parameter μ, in electric voltage $(V_0 = 0, 1)$, coefficient of dimensionless magnetic field $(H_x = 0, 1)$, maximum transverse amplitude $(w_{1\,max} = 1)$ and the viscoelastic damping coefficient $(g = 0.01)$

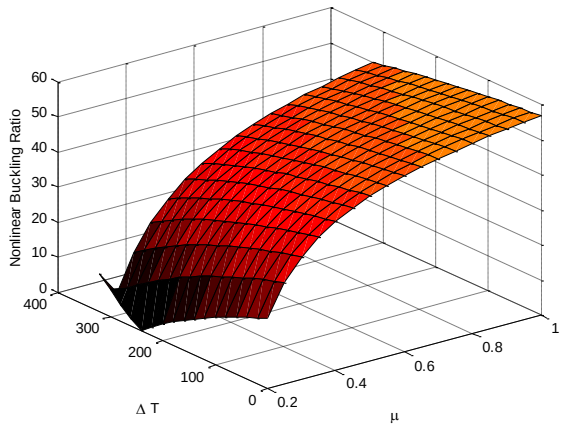

$(V_0 = 0\,, \quad H_x = 1)$

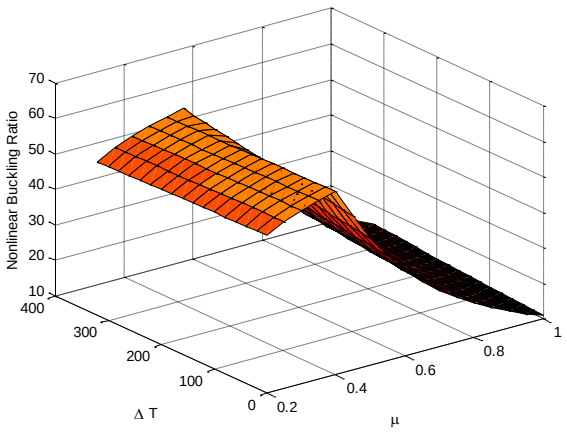

$(V_0 = 1\,, \quad H_x = 1)$

Fig. 11 nonlinear buckling ratio for various values of (ΔT) against nonlocal parameter μ, in electric voltage $(V_0 = 0, 1)$, coefficient of dimensionless magnetic field $(H_x = 0, 1)$, maximum transverse amplitude $(w_{1\,max} = 1)$ and the viscoelastic damping coefficient $(g = 0.01)$

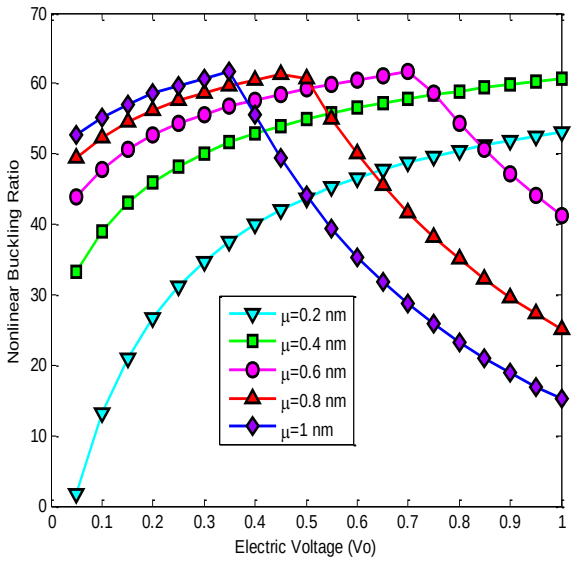

$(\Delta T = 100\ K\ ,\quad H_x = 0)$

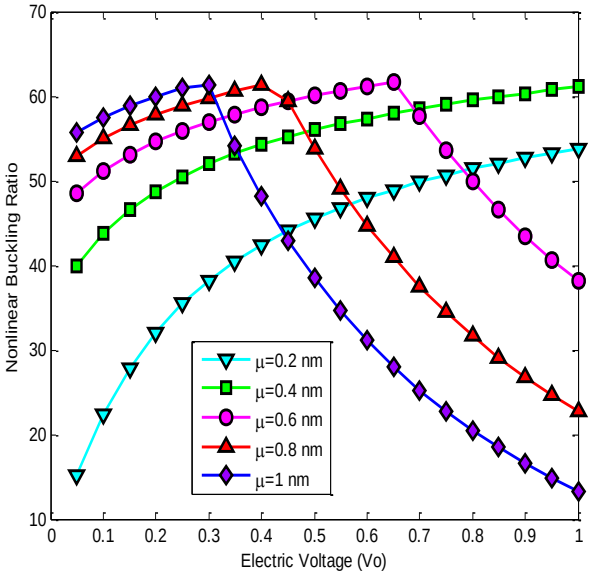

$(\Delta T = 100\ K\ ,\quad H_x = 1)$

Fig. 12 nonlinear buckling ratio for various values of (V_0) against nonlocal parameter μ, in temperature $(\Delta T = 100\ K)$, coefficient of dimensionless magnetic field $(H_x = 0, 1)$, maximum transverse amplitude $(w_{1\,max} = 1)$ and the viscoelastic damping coefficient $(g = 0.01)$

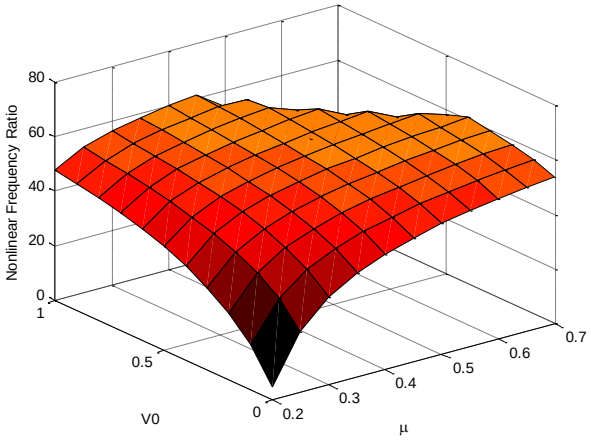

Fig. 13 nonlinear buckling ratio for various values of (V_0) and nonlocal parameter μ, in temperature $(\Delta T = 100\ K)$, coefficient of dimensionless magnetic field $(H_x = 0, 1)$, maximum transverse amplitude $(w_{1\,max} = 1)$ and the viscoelastic damping coefficient $(g = 0.01)$.

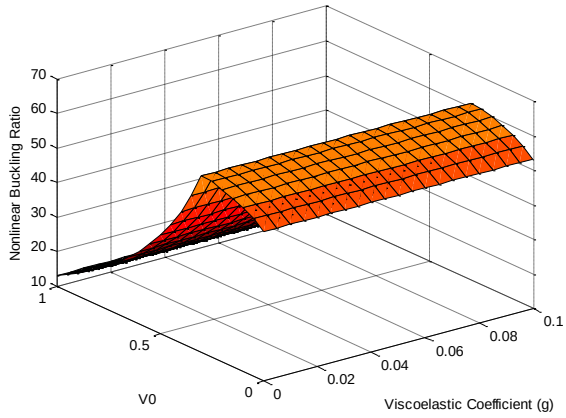

Fig. 14 nonlinear buckling ratio for various values of (V_0) and the viscoelastic damping coefficient (g) in nonlocal parameter $(\mu = 1\,nm)$, temperature $(\Delta T = 100\ K)$, coefficient of dimensionless magnetic field $(H_x = 1)$ and maximum transverse amplitude $(w_{1\,max} = 1)$

derived through Hamilton's principle and the semi-analytical GDQ method are used to discretize the governing equation and associated boundary conditions. Eringen's nonlocal elasticity theory considers the effect of small size, which enables the present model to become effective in the analysis and design of nano-electromechanical systems. Based on Kelvin-Voigt model, the influence of the viscoelastic coefficient is also discussed. It is demonstrated that the GDQ method has high precision and computational efficiency in the vibration analysis of viscoelastic nanoplates. To present a better imagination of the trend of variations of the nonlinear buckling behavior of PZT-4 nanoplate, results are also plotted 3 dimensions. Novelties of the present research are listed at the end of the introduction section.

The main practical conclusions may be summarized as:

- Present results are accurate and in an excellent agreement with results of the nonlocal linear solutions available in literature.
- Increasing the magnetic field, can nonlinearly decreases or increases the buckling load of the viscoelastic double-piezo nanoplates.

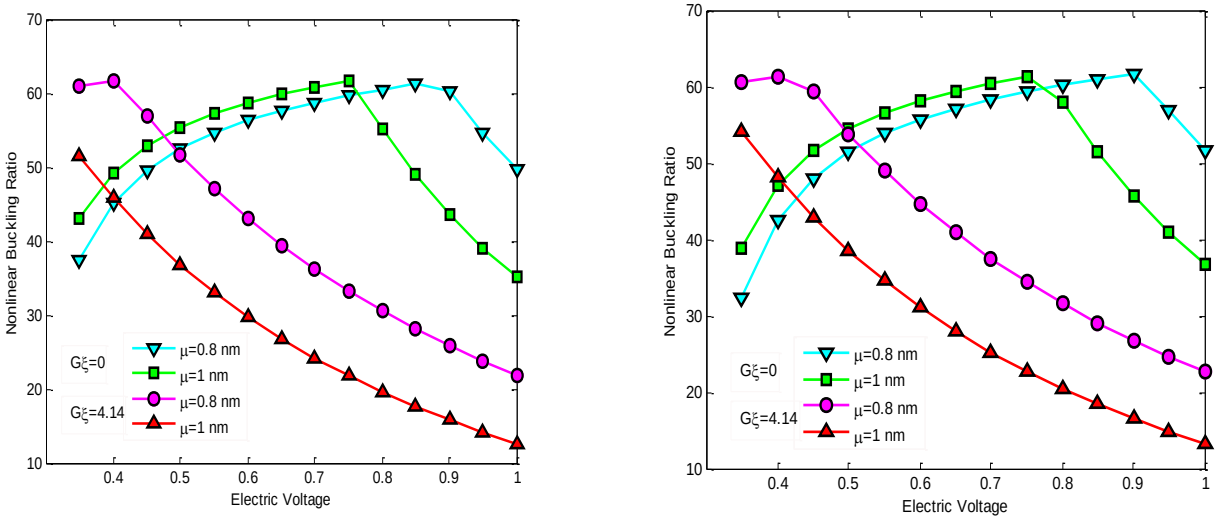

$(\Delta T = 0\,K\,, \quad H_x = 0)$ $(\Delta T = 100\,K\,, \quad H_x = 1)$

Fig. 15 nonlinear buckling ratio for various values of $(G_\xi = 0,\ 4.14)$, nonlocal parameter $(\mu = 0.8\,nm, 1\,nm)$ against electric voltage (V_0) for coefficient of dimensionless magnetic field $(H_x = 0, 1)$, temperature $(\Delta T = 0\,K,\ 100\,K)$ in maximum transverse amplitude $(w_{1\,max} = 1)$ and the viscoelastic damping coefficient $(g = 0.01)$.

• When the small-scale effect increases the hardening stiffness of the nanoplate rapidly decreases. i.e. the small-scale effect makes the nanoplate more flexible.

• Increasing the external electric voltage, considerably and non-monotonically increase the nonlinear buckling load of the viscoelastic double-piezo nanoplates.

• Influence of the small scale is more remarkable for nanoplates with simple supports in all sides and an elastomeric foundation.

• The nonlinear buckling behavior is dependent on many factors, among them: viscoelastic coefficient, magnetic intensity, aspect ratio, material properties and boundary conditions.

• Numerical results are presented to serve as benchmarks for next analyses of viscoelastic piezo nanoplates as fundamental elements in nano thermo-electro-mechanical systems.

References

Ansari, R., Rouhi, H. and Sahmani, S. (2011), "Thermal effect on axial buckling behavior of multi-walled carbon nanotubes based on nonlocal shell model", *Physica E Low Dimensional Syst. Nanostruct.*, **44**(2), 373-378. https://doi.org/10.1016/j.physe.2011.08.036.

Arani, A. G. and Zarei, M. S. H. (2014), "Nonlinear nonlocal vibration of an embedded viscoelastic Y-SWCNT conveying viscous fluid under magnetic field using homotopy analysis method", *J. Solid Mech.*, **6**(2), 173-193.

Arani, A. G., Amir, S., Dashti, P. and Yousefi, M. (2014), "Flow-induced vibration of double bonded visco-CNTs under magnetic fields considering surface effect", *Comput. Mater. Sci.*, **86**, 144-154. https://doi.org/10.1016/j.commatsci.2014.01.047.

Arani, A. G., Kolahchi, R., Barzoki, A. A. M., Mozdianfard, M. R. and Farahani, S. M. N. (2013), "Elastic foundation effect on nonlinear thermo-vibration of embedded double-layered orthotropic graphene sheets using differential quadrature method", *Proc. Institution of Mechanical Engineers, Part C J. Mech. Eng. Sci.*, **227**(4), 862-879. https://doi.org/10.1177/0954406212453808.

Armaghani, D. J., Mirzaei, F., Shariati, M., Trung, N. T., Shariat, M. and Trnavac, D. (2020), "Hybrid ANN-based techniques in predicting cohesion of sandy-soil combined with fiber", *Geomech. Eng.*, **20**(3), 175-189. https://doi.org/10.12989/gae.2020.20.3.175.

Chahnasir, E. S., Zandi, Y., Shariati, M., Dehghani, E., Toghroli, A., Mohamad, E. T., Shariati, A., Safa, M., Wakil, K. and Khorami, M. (2018), "Application of support vector machine with firefly algorithm for investigation of the factors affecting the shear strength of angle shear connectors", *Smart Struct. Syst.*, **22**(4), 413-424. https://doi.org/10.12989/sss.2018.22.4.413.

Chattopadhyay, A. and Gu, H. (1994), "New higher order plate theory in modeling delamination buckling of composite laminates", *AIAA J.*, **32**(8), 1709-1716. https://doi.org/10.2514/3.12163.

Chen, W., Shu, C., He, W. and Zhong, T. (2000), "The application of special matrix product to differential quadrature solution of geometrically nonlinear bending of orthotropic rectangular plates", *Comput. Struct.*, **74**(1), 65-76. https://doi.org/10.1016/S0045-7949(98)00320-4.

Chuanhua, X., Zhang, X., James H. Haido, Peyman Mehrabi, Ali Shariati, Edy Tonnizam Mohamad, Nguyen Hoang and Karzan Wakil, "Using genetic algorithms method for the paramount design of reinforced concrete structures", *Struct. Eng. Mech.*, **71**(5), 503-513. https://doi.org/10.12989/sem.2019.71.5.503.

Di Sciuva, M. (1986), "Bending, vibration and buckling of simply supported thick multilayered orthotropic plates: an evaluation of a new displacement model", *J. Sound Vib.*, **105**(3), 425-442. https://doi.org/10.1016/0022-460X(86)90169-0.

Dickinson, S. M. (1978), "The buckling and frequency of flexural vibration of rectangular isotropic and orthotropic plates using Rayleigh's method", *J. Sound Vib.*, **61**(1), 1-8. https://doi.org/10.1016/0022-460X(78)90036-6.

Eringen, A. C. (1972), "Nonlocal polar elastic continua", *J. Eng. Sci.*, **10**(1), 1-16. https://doi.org/10.1016/0020-7225(72)90070-5.

Eringen, A. C. (1983), "On differential equations of nonlocal elasticity and solutions of screw dislocation and surface

waves", *J. Appl. Phys.*, **54**(9), 4703-4710. https://doi.org/10.1063/1.332803.

Findley, W. N., Lai, J. S. Y. and Onaran, K., (1976), *Creep and Relaxation of Nonlinear Viscoelastic Materials, with an Introduction to Linear Viscoelasticity*, Oxford, New York.

Jamalpoor, A. and Hosseini, M. (2015), "Biaxial buckling analysis of double-orthotropic microplate-systems including in-plane magnetic field based on strain gradient theory", *Compos. Part B Eng.*, **75**, 53-64. https://doi.org/10.1016/j.compositesb.2015.01.026.

Javaheri, R. and Eslami, M. R. (2002), "Thermal buckling of functionally graded plates", *AIAA J.*, **40**(1), 162-169. https://doi.org/10.2514/2.1626.

Jomehzadeh, E. and Saidi, A. R. (2011), "The small scale effect on nonlinear vibration of single layer graphene sheets", *World Acad. Sci. Eng. Technol*, **5**, 235-239.

Jung, W. Y., Han, S. C. and Park, W. T. (2014), "A modified couple stress theory for buckling analysis of S-FGM nanoplates embedded in Pasternak elastic medium", *Compos. Part B Eng.*, **60**, 746-756. https://doi.org/10.1016/j.compositesb.2013.12.058.

Kane, C. L. and Mele, E. J. (1997), "Size, shape, and low energy electronic structure of carbon nanotubes", *Phys. Rev. Lett.*, **78**(10), 1932. https://doi.org/10.1103/PhysRevLett.78.1932.

Kapania, R. K. and Yang, T. Y. (1987), "Buckling, postbuckling, and nonlinear vibrations of imperfect plates", *AIAA J.*, **25**(10), 1338-1346. https://doi.org/10.2514/3.9788.

Katebi, J., Shoaei-parchin, M., Shariati, M., Trung, N. T., & Khorami, M. (2019), "Developed comparative analysis of metaheuristic optimization algorithms for optimal active control of structures", *Eng. Comput.*, 1-20. https://doi.org/10.1007/s00366-019-00780-7.

Ke, L. L. and Wang, Y. S. (2012), "Thermoelectric-mechanical vibration of piezoelectric nanobeams based on the nonlocal theory", *Smart Mater. Struct.*, **21**(2), 025018. https://doi.org/10.1088/0964-1726/21/2/025018.

Knightly, G. H. and Sather, D. (1974), "Nonlinear buckled states of rectangular plates", *Arch. Rational Mech. Anal.*, **54**(4), 356-372. https://doi.org/10.1007/BF00249196.

Kolahchi, R., Bidgoli, M. R., Beygipoor, G. and Fakhar, M. H. (2015), "A nonlocal nonlinear analysis for buckling in embedded FG-SWCNT-reinforced microplates subjected to magnetic field", *J. Mech. Sci. Technol.*, **29**(9), 3669-3677. https://doi.org/10.1007/s12206-015-0811-9.

Kutlu, A. and Omurtag, M. H. (2012), "Large deflection bending analysis of elliptic plates on orthotropic elastic foundation with mixed finite element method", *J. Mech. Sci.*, **65**(1), 64-74. https://doi.org/10.1016/j.ijmecsci.2012.09.004.

Lakes, R., (2009), *Viscoelastic Materials*, Cambridge, New York.

Lancaster, P. and Tismenetsky, M. (1985), *The Theory of Matrices: with Applications*, Elsevier, Germany.

Lei, Z. X., Liew, K. M. and Yu, J. L. (2013), "Buckling analysis of functionally graded carbon nanotube-reinforced composite plates using the element-free kp-Ritz method", *Compos. Struct.*, **98**, 160-168. https://doi.org/10.1016/j.compstruct.2012.11.006.

Li, S. R., Zhou, Y. H. and Song, X. (2002), "Non-linear vibration and thermal buckling of an orthotropic annular plate with a centric rigid mass", *J. Sound Vib.*, **251**(1), 141-152. https://doi.org/10.1006/jsvi.2001.3987.

Li, Y. S., Cai, Z. Y. and Shi, S. Y. (2014), "Buckling and free vibration of magnetoelectroelastic nanoplate based on nonlocal theory", *Compos. Struct.*, **111**, 522-529. https://doi.org/10.1016/j.compstruct.2014.01.033.

Liu, C., Ke, L. L., Wang, Y. S., Yang, J. and Kitipornchai, S. (2013), "Thermo-electro-mechanical vibration of piezoelectric nanoplates based on the nonlocal theory", *Compos. Struct.*, **106**, 167-174. https://doi.org/10.1016/j.compstruct.2013.05.031.

Luo, Z., Sinaei, H., Ibrahim, Z., Shariati, M., Jumaat, Z., Wakil, Pham, Binh Thai, Mohamad, E.T. and Khorami, M. (2019) "Computational and experimental analysis of beam to column joints reinforced with CFRP plates", *Steel Compos. Struct.*, **30**(3), 271-280. https://doi.org/10.12989/scs.2019.30.3.271.

Ma, L. S. and Wang, T. J. (2003), "Nonlinear bending and post-buckling of a functionally graded circular plate under mechanical and thermal loadings", *J. Solids Struct.*, **40**(13-14), 3311-3330. https://doi.org/10.1016/S0020-7683(03)00118-5.

Maiti, A., Svizhenko, A. and Anantram, M. P. (2002), "Electronic transport through carbon nanotubes: Effects of structural deformation and tube chirality", *Phys. Review Lett.*, **88**(12), 126805. https://doi.org/10.1103/PhysRevLett.88.126805.

Mansouri, I., Shariati, M., Safa, M., Ibrahim, Z., Tahir, M. M. and Petković, D. (2019), "Analysis of influential factors for predicting the shear strength of a V-shaped angle shear connector in composite beams using an adaptive neuro-fuzzy technique", *J. Intelligent Manufact.*, **30**(3), 1247-1257. https://doi.org/10.1007/s10845-017-1306-6.

Milovancevic, M., Marinović, J. S., Nikolić, J., Kitić, A., Shariati, M., Trung, N. T., Wakil, K. and Khorami, M. (2019). "UML diagrams for dynamical monitoring of rail vehicles", *Physica A Statistical Mech. Appl.,* **53**, 121169. https://doi.org/10.1016/j.physa.2019.121169.

Mohammadhassani, M., Saleh, A., Suhatril, M. and Safa, M. (2015), "Fuzzy modelling approach for shear strength prediction of RC deep beams", *Smart Struct. Syst.*, **16**(3), 497-519. https://doi.org/10.12989/sss.2015.16.3.497.

Mohammadhassani, M., Nezamabadi-Pour, H., Suhatril, M. and Shariati, M. (2013), "Identification of a suitable ANN architecture in predicting strain in tie section of concrete deep beams", *Struct. Eng. Mech*, **46**(6), 853-868. http://dx.doi.org/10.12989/sem.2013.46.6.853.

Moon, F. C. and Pao, Y. H. (1968), "Magnetoelastic buckling of a thin plate", *J. Appl. Mech.*, **35**(1), 53-58. https://doi.org/10.1115/1.3601173.

Murmu, T. and Pradhan, S. C. (2009), "Buckling of biaxially compressed orthotropic plates at small scales", *Mech. Res. Communications*, **36**(8), 933-938.

Murmu, T., Sienz, J., Adhikari, S. and Arnold, C. (2013), "Nonlocal buckling of double-nanoplate-systems under biaxial compression", *Compos. Part B Eng.*, **44**(1), 84-94. https://doi.org/10.1016/j.compositesb.2012.07.053.

Pietrzakowski, M. (2008), "Piezoelectric control of composite plate vibration: Effect of electric potential distribution", *Comput. Struct.*, **86**(9), 948-954. https://doi.org/10.1016/j.compstruc.2007.04.023.

Pradhan, S. C. and Murmu, T. (2010), "Small scale effect on the buckling analysis of single-layered graphene sheet embedded in an elastic medium based on nonlocal plate theory", *Physica E Low Dimensional Syst. Nanostruct.*, **42**(5), 1293-1301. https://doi.org/10.1016/j.physe.2009.10.053.

Reddy, J. N. (2010), "Nonlocal nonlinear formulations for bending of classical and shear deformation theories of beams and plates", *J. Eng. Sci.*, **48**(11), 1507-1518. https://doi.org/10.1016/j.ijengsci.2010.09.020.

Reddy, J. N. and Wang, C. M. (2004), "Dynamics of fluid-conveying beams: governing equations and finite element models", CORE Report No. 2004-03; Centre for Offshore Research and Engineering, Singapore.

Sedghi, Y., Zandi, Y., Toghroli, A., Safa, M., Mohamad, E. T., Khorami, M. and Wakil, K. "Application of ANFIS technique on performance of C and L shaped angle shear connectors", *Smart Struct. Syst.*, **22**(3), 335-340. https://doi.org/10.12989/sss.2018.22.3.335.

Shahabi, S. E. M., Sulong, N. H., Shariati, M., Mohammadhassani, M. and Shah, S. N. R. (2016), "Numerical analysis of channel connectors under fire and a comparison of performance with different types of shear connectors subjected to fire", *Steel Compos.*

Struct., **20**(3), 651-669. https://doi.org/10.12989/scs.2016.20.3.651.
Shahwan, K. W. and Waas, A. M. (1998), "Buckling of unilaterally constrained plates: applications to the study of delaminations in layered structures", *J. Franklin Institute*, **335**(6), 1009-1039. https://doi.org/10.1016/S0016-0032(97)00053-7.
Shao, Z., Armaghani, D. J., Bejarbaneh, B. Y., Mu'azu, M. and Mohamad, E. T. (2019a), "Estimating the Friction Angle of Black Shale Core Specimens with Hybrid-ANN Approaches", *Measurement*, **145**, https://doi.org/10.1016/j.measurement.2019.06.007.
Shao, Z., Gholamalizadeh, E., Boghosian, A., Askarian, B. and Liu, Z. (2019b). "The chiller's electricity consumption simulation by considering the demand response program in power system", *Appl. Therm. Eng.,* **149**, 1114-1124. https://doi.org/10.1016/j.applthermaleng.2018.12.121.
Shao, Z. and Vesel, A. (2015). "Modeling the packing coloring problem of graphs", *Appl. Math. Model.,* **39**(13), 3588-3595. https://doi.org/10.1016/j.apm.2014.11.060.
Shao, Z., Wakil, K., Usak, M., Amin Heidari, M., Wang, B. and Simoes, R. (2018), "Kriging Empirical Mode Decomposition via support vector machine learning technique for autonomous operation diagnosing of CHP in microgrid", *Appl. Thermal. Eng.,* **145**, 58-70. https://doi.org/10.1016/j.applthermaleng.2018.09.028.
Shariati, A., Ebrahimi, F., Karimiasl, M., Vinyas, M. and Toghroli, A. (2020a), "On transient hygrothermal vibration of embedded viscoelastic flexoelectric/piezoelectric nanobeams under magnetic loading", *Adv. Nano. Res*., **8**(1), 49-58. https://doi.org/10.12989/anr.2020.8.1.049
Shariati, M., Ghorbani, M., Naghipour, M., Alinejad, N. and Toghroli, A. (2020b), "The effect of RBS connection on energy absorption in tall buildings with braced tube frame system", *Steel Compos. Struct.* **34**(3), 393-407. https://doi.org/10.12989/scs.2020.34.3.393.
Shariati, M., Mafipour, M. S., Haido, J. H., Yousif, S. T., Toghroli, A., Trung, N. T. and Shariati, A. (2020c), "Identification of the most influencing parameters on the properties of corroded concrete beams using an Adaptive Neuro-Fuzzy Inference System (ANFIS)", *Steel Compos. Struct.* **34**(1), 155. https://doi.org/10.12989/scs.2020.34.1.155.
Shariati, M., Mafipour, M. S., Mehrabi, P., Ahmadi, M., Wakil, K., Nguyen-Thoi, T. and Toghroli, A. (2020d), "Prediction of concrete strength in presence of furnace slag and fly ash using Hybrid ANN-GA (Artificial Neural Network-Genetic Algorithm)", *Smart Struct. Syst.,* **25**(2), 183-195. https://doi.org/10.12989/sss.2020.25.2.183.
Shariati, M., Mafipour, M. S., Mehrabi, P., Bahadori, A., Zandi, Y., Salih, M. N. A., Nguyen, H., Dou, J., Song, X. and Poi-Ngian, S. (2019a), "Application of a Hybrid Artificial Neural Network-Particle Swarm Optimization (ANN-PSO) Model in Behavior Prediction of Channel Shear Connectors Embedded in Normal and High-Strength Concrete", *Appl. Sci*., **9**(24), 5534.
Shariati, M., Mafipour, M.S., Mehrabi, P., Shariati, A., Toghroli, A., Trung, N.T. and Salih, M.N.A. (2020e), "A novel approach to predict shear strength of tilted angle connectors using artificial intelligence techniques", *Eng. Comput.*, 1-21. https://doi.org/10.1007/s00366-019-00930-x.
Shariati, M., Mafipour, M. S., Mehrabi, P., Zandi, Y., Dehghani, D., Bahadori, A., Shariati, A., Trung, N.T., Salih, M.N.A. and Poi-Ngian, S. (2019), "Application of Extreme Learning Machine (ELM) and Genetic Programming (GP) to design steel-concrete composite floor systems at elevated temperatures", *Steel Compos. Struct.*, **33**(3), 319-332. https://doi.org/10.12989/scs.2019.33.3.319.
Shariati, M., Naghipour, M., Yousofizinsaz, G., Toghroli, A. and Pahlavannejad Tabarestani, N. (2020f), "Numerical study on the axial compressive behavior of built-up CFT columns considering different welding lines", *Steel Compos. Struct.* **34**(3), 377-391.https://doi.org/10.12989/scs.2020.34.3.377.
Shariati, M., Trung, N. T., Wakil, K., Mehrabi, P., Safa, M. and Khorami, M. (2019), "Moment-rotation estimation of steel rack connection using extreme learning machine", *Steel. Compos. Struct*., **31**(5), 427-435. https://doi.org/10.12989/sem.2019.70.5.639.
Shi, X., Hassanzadeh-Aghdam, M. and Ansari, R. (2019a), "Viscoelastic analysis of silica nanoparticle-polymer nanocomposites", *Compos. Part B Eng.,* **158**, 169-178. https://doi.org/10.1016/j.compositesb.2018.09.084.
Shi, X., Jaryani, P., Amiri, A., Rahimi, A. and Malekshah, E. H. (2019b), "Heat transfer and nanofluid flow of free convection in a quarter cylinder channel considering nanoparticle shape effect", *Powder Technol*., **346**, 160-170. https://doi.org/10.1016/j.powtec.2018.12.071.
Shen, H. S. (2000), "Nonlinear bending of shear deformable laminated plates under transverse and in-plane loads and resting on elastic foundations", *Compos. Struct.*, **50**(2), 131-142. https://doi.org/10.1016/S0263-8223(00)00088-X.
Shen, H. S. (2009), "Nonlinear bending of functionally graded carbon nanotube-reinforced composite plates in thermal environments", *Compos. Struct.*, **91**(1), 9-19. https://doi.org/10.1016/j.compstruct.2009.04.026.
Swaminathan, K. and Ragounadin, D. (2004), "Analytical solutions using a higher-order refined theory for the static analysis of antisymmetric angle-ply composite and sandwich plates", *Compos. Struct.*, **64**(3-4), 405-417. https://doi.org/10.1016/j.compstruct.2003.09.042.
Suhatril, M., Osman, N., Sari, P. A., Shariati, M. and Marto, A. (2019), "Significance of Surface Eco-Protection Techniques for Cohesive Soils Slope in Selangor, Malaysia", *Geotech. Geological Eng*., **37**(3), 2007-2014. https://doi.org/10.1007/s10706-018-0740-3.
Trung, N. T., Shahgoli, A. F., Zandi, Y., Shariati, M., Wakil, K., Safa, M. and Khorami, M. (2019), "Moment-rotation prediction of precast beam-to-column connections using extreme learning machine", *Struct. Eng. Mech.*, **70**(5), 639-647. https://doi.org/10.12989/sem.2019.70.5.639.
Wang, Q. (2002), "Axi-symmetric wave propagation in a cylinder coated with a piezoelectric layer", *J. Solids Struct.*, **39**(11), 3023-3037. https://doi.org/10.1016/S0020-7683(02)00233-0.
Zhang, J., Wang, C. and Chen, W. (2014), "Surface and piezoelectric effects on the buckling of piezoelectric nanofilms due to mechanical loads", *Meccanica*, **49**(1), 181-189. https://doi.org/10.1007/s11012-013-9784-x.
Zhao, M., Qian, C., Lee, S. W. R., Tong, P., Suemasu, H. and Zhang, T. Y. (2007), "Electro-elastic analysis of piezoelectric laminated plates", *Adv. Compos. Mater.*, **16**(1), 63-81. https://doi.org/10.1163/156855107779755273.
Žiliukas, A. (2008), "Plate buckling under complex loading", *Mechanics,* **74**(6), 17-20.
Zong, Z. and Zhang, Y. (2009), *Advanced Differential Quadrature Methods*, Chapman and Hall/CRC Press, Florida, U.S.A.

CC